

# EStreams: An integrated dataset and catalogue of streamflow, hydro-climatic and landscape variables for Europe

## Authors

Thiago V. M. do Nascimento<sup>1,3</sup>, Julia Rudlang<sup>2</sup>, Marvin Höge<sup>1</sup>, Ruud van der Ent<sup>2</sup>, Máté Chappon<sup>4</sup>, Jan Seibert<sup>3</sup>, Markus Hrachowitz<sup>2</sup> and Fabrizio Fenicia<sup>1</sup>

## Affiliations

1. Eawag: Swiss Federal Institute of Aquatic Science and Technology, Dübendorf, Switzerland
2. Department of Water Management, Faculty of Civil Engineering and Geosciences, Delft University of Technology, Delft, Netherlands
3. Department of Geography, University of Zurich, Zurich, Switzerland
4. Széchenyi István University, Department of Transport Infrastructure and Water Resources Engineering, Győr, Hungary

corresponding author: Thiago Nascimento (thiago.nascimento@eawag.ch)

**THIS IS A NON-PEER REVIEWED PREPRINT.**

## Abstract

Large-sample hydrology datasets have become increasingly available, contributing to significant scientific advances. However, in Europe, only a few such datasets have been published, capturing only a fraction of the wealth of information from national data providers in terms of available spatial density and temporal extent. We present “EStreams”, an extensive dataset of hydro-climatic variables and landscape descriptors and a catalogue of openly available stream records for 17,130 European catchments. Spanning up to 120 years, the dataset includes streamflow indices, catchment-aggregated hydro-climatic signatures and landscape attributes (topography, soils, geology, vegetation and landcover). The catalogue provides detailed descriptions that allow users to directly access streamflow data sources, overcoming challenges related to data redistribution policies, language barriers and varied data portal structures. EStreams also provides Python scripts for data retrieval, aggregation and processing, making it dynamic in contrast to static datasets. This approach enables users to update their data as new records become available. Our goal is to extend current large-sample datasets and further integrate hydro-climatic and landscape data across Europe.

## Background & Summary

Large-sample datasets of hydrological variables across many catchments and long time periods are crucial for understanding and predicting hydrological variability in time and space<sup>1,2</sup>. These datasets are increasingly in demand due to the rise of data-intensive machine learning models<sup>3</sup>.

Following the publication of the MOPEX dataset in the early 2000s, there has recently been a broad movement to making large-sample hydrology (LSH) datasets available. Many of those were developed inspired by the Catchment Attributes and MEteorology for Large-sample Studies (CAMELS) initiative that compiled and made available full datasets for the contiguous United States<sup>1</sup>. Many countries and regions have embraced these or similar initiatives, including Australia<sup>4</sup>, Brazil<sup>5</sup>, Chile<sup>6</sup>, Great Britain<sup>2</sup>, Switzerland<sup>7</sup>, Central-Europe<sup>8</sup>, North America<sup>9</sup>, China<sup>10</sup>, Central Asia<sup>11</sup> and Iceland<sup>12</sup>.

At the global scale, there are already some collection efforts for hydro-meteorological data. The Global Streamflow Indices and Metadata Archive (GSIM)<sup>13,14</sup> provides streamflow

49 indices for 35,000+ locations around the globe, but no extensive set of catchment landscape  
50 and meteorological attributes. Recently another global streamflow indices time series  
51 initiative took place enlarging the analysis to 41,000+ river branches worldwide and using  
52 different streamflow signatures to enrich the flow regime analysis<sup>15</sup>. Considering streamflow  
53 records, the Global Runoff Data Centre (GRDC)<sup>16</sup> provides data for 10,000+ stations, but similar  
54 to the previous datasets, no catchment attributes and meteorological forcing time series are  
55 available. In addition, the GRDC data is only updated episodically, while the others do, to our  
56 knowledge, not provide any updates. More recently the Caravan<sup>3</sup> dataset compilation was  
57 published as a global initiative for standardizing already open-source published streamflow  
58 datasets of initially 6,830 catchments, where catchment attributes and meteorological forcing  
59 were derived from gridded global products.

60 While global datasets offer easy access, they come with limitations. Firstly, their  
61 spatial coverage remains restricted, offering only a fraction of data available from national  
62 providers worldwide. The Caravan dataset, for example, originally covered Europe for only  
63 Great Britain, Austria and the Danube catchment as far downstream as the city of Bratislava  
64 (Slovakia). By now, there are multiple extensions for Denmark, Israel, Switzerland, Spain,  
65 Iceland and, most recently, a GRDC extension<sup>17</sup> adding another 25 countries globally. Yet, for  
66 eastern and southern Europe publicly available data is still difficult to access. Secondly, such  
67 datasets are also limited in their temporal extent. For example, the CAMELS-GB<sup>2</sup> covers the  
68 period from 1970 to 2015, while the LamaH-CE dataset<sup>11</sup> spans from 1981 to 2017. Thirdly,  
69 existing large sample hydrology datasets, including the CAMELS databases, lack extensibility,  
70 making the accommodation of newly available data challenging.

71 Although most countries collect daily streamflow data at numerous river gauging  
72 stations, compiling a comprehensive hydrological dataset from this information presents  
73 significant challenges. Firstly, access to these data can be challenging. Some countries offer  
74 this data on the official websites of government agencies or associated data providers, while  
75 others provide it upon request. Official government websites are frequently available only in  
76 national languages, adding an extra layer of complexity. Gaining access can be intricate,  
77 involving navigation to a selection of stations and periods, which need to be downloaded  
78 individually. Secondly, substantial formatting and pre-processing are often necessary before  
79 the data can be effectively utilized. Finally, redistribution restrictions may hinder the  
80 republishing of country-specific data. These obstacles pose significant barriers to hydrological  
81 analyses of catchments in large-sample investigations, particularly given the short timeframes  
82 of typical research projects.

83 Here, we present “EStreams”, a platform consisting of two distinct products: (1) an  
84 extensive streamflow catalogue together with Python scripts for data direct access at the  
85 individual data providers and (2) a dataset of weekly, monthly, seasonal and annual indices, of  
86 streamflow, together with the associated catchment-averaged hydro-climatic signatures,  
87 meteorological time series and landscape descriptors for 17,130 catchments across 41  
88 countries over pan-European territory. Currently, the dataset covers the period of 1900-2022.

89 While the focus of EStreams is on streamflow, the EStreams dataset also contains  
90 catchment aggregated meteorological forcing and landscape descriptors, typically necessary  
91 for hydrological analyses. These indices and descriptors were derived from various open  
92 sources and include climate<sup>18,19</sup>, geology<sup>20,21</sup>, hydrology and topography<sup>22-25</sup>, land use and land  
93 cover<sup>26-28</sup>, soil types<sup>29-31</sup> and vegetation characteristics<sup>32,33</sup>. Similarly to streamflow, national  
94 providers often have more accurate information for such auxiliary data, but seldom they are  
95 easily accessible.

96 Unlike existing global datasets, which are relatively “static” as not easily updatable  
97 with new stations or recent time periods, EStreams is designed as “dynamic” by linking users  
98 to the original data providers. While “static” datasets may offer more accurate quality checks  
99 and are well-suited for applications such as benchmarking methods and models, many  
100 practical applications benefit from using the most up-to-date and dense data. This is  
101 particularly true for tasks like accurate streamflow predictions using data-intensive machine  
102 learning models.

103 Hence, our main contributions with this work are:

- 104 i. Introducing the most extensive and extensible integrated collection of weekly,  
105 monthly, seasonal and annual indices of streamflow for Europe, along with  
106 catchment-aggregated meteorological and landscape variables (dataset).
- 107 ii. Providing detailed metadata for streamflow gauges, including catchment boundaries,  
108 and a catalogue of the corresponding data providers.
- 109 iii. Allowing reproducibility and extension by making available all codes used to retrieve  
110 the source data and aggregate them by catchment in an easy-to-use workflow,  
111 allowing users to directly and readily access the desired data from data providers.

112 The methodology employed to process the source data and obtain the current dataset and  
113 catalogue is illustrated in **Figure 1**. This figure highlights the primary data sources, the general  
114 procedure, and the final outputs of EStreams. A detailed description of each step is provided  
115 in the Methods sections.

## 116 **Methods**

### 117 **Streamflow data**

#### 118 **Available stations**

119 Daily streamflow data from 17,130 European river catchments with varying sizes and  
120 characteristics were aggregated from 41 countries and more than 50 different data providers.  
121 In some countries, such as Italy and Germany, multiple data providers contributed to the  
122 dataset. **Figure 2a** shows the distribution of the gauges with their respective catchment  
123 boundaries in the background. As can be seen in the figure, there is a significant variability in  
124 terms of station density, which is the highest in central Europe and the lowest in the South  
125 and the East. The time series records span the period 1900–2022, with varying length for each  
126 catchment, as shown in **Figure 2b**. Central Europe features the longest time series, with many  
127 stations with records extending over 80 years. **Figure 2c** shows the evolution of the number  
128 of stations with measurements at a given time accounting for the discontinuity of stations over  
129 time. The plot shows an increasing trend in the number of gauging stations with concurrent  
130 records.

131 The streamflow records were selected based on the following criteria: (i) they were  
132 available from official authorities in their respective country or from a recent open-access  
133 dataset, and (ii) they were open-source and easily accessible either via the internet or by e-  
134 mail request. The latter point emphasizes that no dataset requiring purchase for non-  
135 commercial access were included. It is important to note that freely available data do not  
136 necessarily come with a free redistribution license. Therefore, we cannot and do not make raw  
137 daily streamflow data directly available. Should the source data be necessary, we provide the  
138 EStreams catalogue of data sources to allow users easy and direct data access from the original  
139 repositories, including codes and instructions for data download and formatting. Compared to  
140 static databases of pre-compiled datasets currently available, our approach has two main  
141 advantages:

- 142 i. Users can tailor the download to determine the desired spatial and temporal  
143 coverage, also making use of the provided descriptive statistics of the source data,  
144 such as regime characteristics or catchment properties.
- 145 ii. Users can access the most up-to-date information directly from the data sources.

146 **Table 1** provides an overview of the contributing countries, the number of streamflow  
147 gauges, and the data providers. France has the highest number of gauges (4,968), followed by  
148 Germany (2,093) and Spain (1,440). In contrast, Bulgaria (8 gauges) Moldova (2) and North  
149 Macedonia (1) have the lowest numbers of gauges.

### 150 **Streamflow gauges labelling**

151 After the collection of the streamflow data and gauge information from each provider, the  
152 individual datasets were collated into a single dataset. In this process, each gauge was labelled  
153 with a unique 8-digit code. Consequently, each catchment was renamed according to its  
154 respective streamflow gauge. The 8-digit codes were generated using the following logic: the  
155 first two digits represent the country/region, the next two digits represent specifications about  
156 the data provider within regions that had more than one official provider, and the last four  
157 digits refer to the gauge counter for each country/region. For example, the gauge GB000045  
158 represents Great Britain (GB), with only one provider (00), and the gauge number 0045.  
159 Similarly, ITIS0001 represents Italy (IT), with ISPRA (IS) as the data provider, and gauge number  
160 0001. The gauges with records obtained from GRDC have the second two digits as “GR” (e.g.,  
161 LVGR0001) to facilitate identification. This standardization ensures that all gauges are  
162 consistently labelled, providing users with a clear indication of the source and the number of  
163 records.

### 164 **Identification of duplicate gauges**

165 When compiling large streamflow datasets, there is a possibility of having duplicate records  
166 within the dataset that need to be identified and removed. This issue can arise when  
167 combining information from multiple sources and even within datasets obtained from a single  
168 data provider. To identify suspected duplicate records, we used a similar approach as used by  
169 the GSIM<sup>13</sup>, where for gauges originating from distinct data providers, we identified potential  
170 duplicate gauges by examining similarities in gauge and river names. We employed the Jaro-  
171 Winkler distance metric to quantify alphanumeric similarity, as discussed by Christen, 2012<sup>34</sup>  
172 with a threshold set at 0.70. We additionally considered spatial proximity, constraining pairs  
173 of stations within 1 km of each other. For gauges originating from the same data provider, we  
174 selected stations within a spatial proximity of 50 m and a delineated area difference below  
175 1%. Gauges meeting these criteria were flagged as potential duplicates. The list of potential  
176 duplicates for each gauge is contained in the attribute ***duplicated\_suspect*** within the gauges'  
177 layer in the final EStreams dataset. Notably, all potential duplicates are preserved in EStreams,  
178 giving users the flexibility to choose their preferred station and data provider when duplicates  
179 are found. This approach ensures that users can tailor their dataset according to their specific  
180 needs and preferences.

### 181 **Quality flags of records**

182 Quality control of streamflow data is essential before undertaking any hydrological study.  
183 While some data providers include quality flags with each published record, this practice is not  
184 consistently available. Automatic checks are available but may be subjective, and their  
185 effectiveness has not yet been fully investigated<sup>35,36</sup>. For example, Do, 2018<sup>13</sup> employed an  
186 automatic detection criterion to identify and filter potentially suspect records based on  
187 negative values, consecutive repetitions, and outliers. However, these filtering criteria are not  
188 always reliable, as pointed out by Chen, 2023<sup>15</sup>.

189 In this work, following the approach utilized by Chen, 2023<sup>15</sup>, we adopt a two stages  
 190 approach for quality checking the data, the first oriented at individual data points, and the  
 191 second assessing the entire record. The first stage is primarily based on the quality flags from  
 192 the original providers, when available, which for consistency are reclassified into four  
 193 categories: “missing”, “no-flags”, “suspect” and “reliable”. First, all negative values were  
 194 replaced with “not a number” (*NaN*) and flagged as “missing”. Then, values with a quality flag  
 195 given by the data providers had their original labels reclassified as either “reliable”, “suspect”  
 196 or “missing”. Finally, all data without a quality flag from the original providers were classified  
 197 as “no-flag”. A complete overview of the mapping between the original flags and our four flags  
 198 system is available in **Supplementary Table 1**.

199 In the second stage, we assessed the overall reliability of each entire time series based  
 200 on the fraction of problematic data points as determined in the previous stage. This  
 201 classification considered five criteria outlined in **Table 2**.

202 A total of 7,430 stations had quality flags from their providers (about 43% of the total).  
 203 **Figure 3a** shows that approximately 134 million data points (63.4% of the total) were classified  
 204 as “no-flag”, 56 million data points (26.7%) as “reliable”, 3.9 million data points (1.9%) as  
 205 “suspect”, and 16.8 million data points (8%) as “missing”. Regarding the gauge’s quality  
 206 classification, **Figure 3b** shows that most stations were categorized as either Class A or B  
 207 (9,652), followed by Class E (3,317), Class C (2,827) and Class D (1,334). This classification  
 208 allows users to filter the data depending on their needs. It is noteworthy that many national  
 209 providers may offer only high-quality data for download. Therefore, even without explicit  
 210 quality flags, the data can often be assumed to come from reliable stations. The quality flag  
 211 for each gauge's records is stored as the attribute *gauge\_flag* within the gauges' layer in the  
 212 final EStreams dataset.

### 213 **Basin delineation**

214 Since catchment boundaries shapefiles were rarely available from national providers, this  
 215 work adopted a semi-automatic delineation of catchment boundaries corresponding to  
 216 streamflow gauges using Python scripts and QGIS software. We used the “delineator” python  
 217 package<sup>37</sup>, which determines catchment boundaries using hybrid vector and raster-based  
 218 methods. This package requires as input the latitude and longitude coordinates of the  
 219 streamflow gauges and uses the MERIT-Hydro Digital Elevation Model (DEM)<sup>22</sup>. MERIT-Hydro  
 220 is a digital elevation model (DEM) developed to remove multiple error components from the  
 221 existing spaceborne DEMs (SRTM3 v2.1 and AW3D-30m v1).

222 To appraise the accuracy of the delineated area, catchments were split into two  
 223 categories: (i) catchments with a reported area from the data providers and (ii) catchments  
 224 without this information. For gauges with available official catchment areas, the reported area  
 225 was compared to the derived area, and the following workflow was adopted:

- 226 i. First, we computed the “relative area difference”  $A_{rel}$  as defined in **Eq. 1**. If  $|A_{rel}|$  was  
 227 below 10%, regardless of catchment size, the delineation was accepted, and the  
 228 catchment was labelled with a quality flag of “0”.
- 229 ii. Otherwise, the catchment delineation was visually inspected, potentially corrected as  
 230 described below, and assigned a specific quality flag as detailed in **Table 3**, which  
 231 provides an overview of the flags used and number of gauges corresponding to each  
 232 flag.

$$A_{rel} = 100 \times \frac{A_{EStreams} - A_{official}}{A_{official}} \quad (1)$$

233 where  $A_{EStream}$  is the calculated area in EStreams and  $A_{official}$  is the reported official area.  
 234 The visual inspection was made using the river networks from both the MERIT-Hydro and EU-  
 235 Hydro datasets<sup>38</sup>, Google Maps satellite imagery, and nearby catchments delineated and  
 236 labelled with a quality flag of “0”. These three data sets were used as they represent

237 independent sources and offer a good trade-off for evaluating the catchment delineation  
238 usability.

239 During the visual inspection, it was observed that some boundary discrepancies could  
240 be corrected with an adjustment in the streamflow gauge location. We assumed that  
241 uncertainties in the georeferenced system or the presence of close-by river branches could  
242 cause these discrepancies. For those catchments, the gauge location was moved (snapped) to  
243 the closest point within the MERIT-Hydro River network based on the gauge's river and  
244 location names.

245 Catchments with  $|A_{rel}|$  below 10% after the snap were labelled with a quality flag "1"  
246 indicating accepted delineation after the snap. The remaining catchments were classified with  
247 the criteria detailed in **Table 3**.

248 It is important to note that for some situations where human-influence such as  
249 canalization, water exports and specific lithologies like karstic systems, the actual catchment  
250 boundary delineation remains challenging. Hence, for catchments where  $|A_{rel}|$  was above 10%  
251 and the visual inspection indicated such situations, we assigned a quality flag of "888".

252 Finally, catchments where  $|A_{rel}|$  was above 10%, and were not visually adjusted or  
253 accepted, were assigned to a quality flag "999".

254 Out of a total of 17,130 stations, 15,775 (92%) had a reported catchment area from  
255 the data providers. **Figure 4a** shows the distribution of these streamflow gauges divided into  
256 two classes: gauges with  $|A_{rel}|$  above 50% (in red), and those with  $|A_{rel}|$  below 50% (in blue).  
257 Generally, gauges with high area discrepancies are located in regions of low relief, partly  
258 canalized landscapes and with high presence of lakes such as in Denmark, Sweden and Croatia.

259 **Figure 4b** shows the exceedance percentage of  $|A_{rel}|$  of these 15,775 catchments with  
260 a reported area. As indicated with the dashed orange line, the catchments with  $|A_{rel}|$  above  
261 50% was 8% (1,205 catchments). This analysis also shows that less than 17% of the catchments  
262 (2,712) had  $|A_{rel}|$  above 10%.

263 **Figure 4c** focuses on catchments with  $|A_{rel}|$  above 50% (1,205 catchments) and shows  
264 how the fraction of these catchment varies with catchment area. Notably, 17% of catchments  
265 under 100 km<sup>2</sup> exhibited  $|A_{rel}|$  above 50%, while in all other ranges shown in the bar plot, the  
266 occurrence was below 5%. This analysis suggests that catchments with significant area  
267 differences tend to be relatively small.

268 Finally, for the 1,355 gauges (8% of the data) without catchment area information, the  
269 delineation was visually inspected, and a label was assigned to indicate the accuracy of the  
270 delineation based on the criteria shown in **Table 3**. Note that as it is not possible to calculate  
271  $|A_{rel}|$  for these catchments, the quality flags of "0" or "1" were never assigned to such basins.  
272 The visual inspection was again made using the river name, the river network provided by  
273 MERIT-Hydro and the EU-Hydro, Google Maps satellite imagery and nearby catchments  
274 delineated and labelled with a quality flag of "0".

275 Hence, in the gauges' layer stored in the final EStreams dataset, besides the original *lat*  
276 and *lon* coordinates, we included the *lat\_snap* and *lon\_snap* coordinates after the potential  
277 snap. The gauges layer also received an attribute called *area\_estreams*, which express the  
278  $A_{Stream}$ . Additionally, we included the  $A_{rel}$  as the attribute *area\_rel*, and the qualitative flag as  
279 the attribute *area\_flag*.

## 280 **Catchment aggregated data**

281 The EStreams dataset includes streamflow, meteorological, and landscape variables. For  
282 streamflow, we distinguish between dynamic streamflow indices and hydro-climatic  
283 signatures, which are further detailed in their respective sections. Meteorological variables  
284 are discussed in the "Meteorological records" section. Finally, landscape attributes were  
285 categorized into six groups (Topography, Soils, Geology, Hydrology, Vegetation, and Land

286 Cover) and are described in the "Landscape attributes" section. All catchment aggregations  
287 were derived using the catchment boundaries and areas calculated by EStreams. For example,  
288 all streamflow indices and signatures were computed using the specific discharge (in mm/day)  
289 derived with the  $A_{EStreams}$  areas.

### 290 **Streamflow indices**

291 In EStreams, streamflow data is presented in terms of "indices", hence statistics of the daily  
292 data such as mean streamflow, maximum, minimum, percentiles and coefficient of variation,  
293 which are provided at annual, seasonal, monthly and weekly resolutions. The use of these  
294 indices is consistent with earlier works, such as the GSIM dataset<sup>13,14</sup> and the  
295 CCI/WCRP/JCOMM Expert Team on Climate Change Detection and Indices (ETCCDI)  
296 (<https://www.wcrp-climate.org/data-etccdi>).

297 The use of indices instead of the daily data allows to make relevant climate  
298 information publicly available in cases where access to raw daily values is restricted. The  
299 selected indices, as discussed in the GSIM dataset<sup>13,14</sup>, are of high relevance and have been  
300 widely used in many hydrological studies, as they can facilitate the analysis of trends and  
301 changes in the regional water balance and the seasonal cycle.

302 The streamflow indices contained in EStreams are presented in **Table 4**, alongside with  
303 their units and temporal resolution. All the indices were computed for time-steps where at  
304 least 95% of the data was available, e.g., at annual time-step, the indices were computed for  
305 years where at least 347 days of data were available.

### 306 **Hydro-climatic signatures**

307 In addition to the streamflow indices, we computed the same set of meteorological and  
308 hydrological signatures provided in the original CAMELS dataset<sup>1</sup>. Unlike streamflow indices,  
309 these signatures were calculated for the entire time period between 1950-2022 where data  
310 are available. Here we refer to these indices and signatures as hydro-climatic signatures (e.g.,  
311 streamflow & precipitation mean, seasonality & aridity index, and runoff coefficient). For  
312 meteorology, we used precipitation and temperature derived from the Ensembles  
313 Observation (E-OBS) product<sup>19</sup>. This work used the "hydroanalysis" python package<sup>39</sup> for the  
314 computation of these signatures.

315 The full list of signatures used is available in **Table 5**. We considered only catchments  
316 with more than one year of continuous measurements within the period of 1950-2022.  
317 Additionally, we also provide the number of years used for the signature's computation  
318 (*num\_years*), the start (*start\_date*) and the end (*end\_date*) of the observations between  
319 1950-2022 to give a further overview of the period the signature refers to, considering  
320 separately the hydrological (*hydro*) and the climatic (*climatic*) signatures.

### 321 **Meteorological records**

322 EStreams used E-OBS<sup>19</sup> for meteorological forcing data records, which has been widely used  
323 in hydrological studies over Europe<sup>40-43</sup>. E-OBS provides a pan-European observational dataset  
324 of surface climate variables that is derived by statistical interpolation of in-situ measurements,  
325 collected from national data providers. It is an open-access database with daily records ranging  
326 from 1950-present. We used the ensemble mean dataset at a resolution of 0.25 degrees.  
327 Additionally, we used the temperature records from E-OBS to derive potential  
328 evapotranspiration (PET) using the Hargreaves formulation<sup>44</sup> and the "pyet" python package<sup>45</sup>  
329 for computation. Each catchment has 9 daily meteorological time series associated with it,  
330 which are illustrated in **Table 6**. The accuracy of E-OBS may be dependent on station density<sup>43</sup>,  
331 which varies across Europe. In order to account for this potential source of uncertainty,  
332 EStreams also includes information on the number of weather stations and density aggregated  
333 to a buffer of 10 km within each catchment boundary.

## 334 Landscape attributes

335 A full overview of the landscape attributes contained in EStreams is shown in **Table 7** and **Table**  
336 **8**, with a short description, their units, and data provider. Regarding spatial coverage, except  
337 for the landcover & land use and soil types that have pan-European coverage, all the remaining  
338 products are global. **Table 7** covers solely the fully static attributes, which are considered time  
339 invariant, such as elevation, soil types, main geology and mean vegetation indices. Conversely,  
340 **Table 8** encompasses a group of attributes that are considered time variable, such as  
341 normalized difference vegetation index (NDVI), leaf-area index (LAI), irrigation and snow  
342 cover. These attributes are reported in time series at either monthly, yearly or in a specific  
343 number of years (e.g., irrigation and landcover) resolution.

344 Topographical attributes were based on MERIT-Hydro<sup>22</sup>. Geology made use of the  
345 widely used Global Lithological Map Database (GLiM)<sup>20</sup> and a gridded product for the  
346 estimation of the depth to bedrock<sup>21</sup>, which have been both used in several applications  
347 databases<sup>1,8,24</sup>. For the number of dams and of total upstream reservoir volume we used the  
348 Georeferenced global dams and reservoirs dataset<sup>23</sup>. A similar aggregation was performed for  
349 lakes using the HydroLakes dataset<sup>46</sup>. Vegetation indices and snow cover percentage made use  
350 of three MODIS products<sup>28,32,33</sup> and were aggregated considering both temporal and static  
351 attributes. For irrigation, we decided to use the global dataset of the extent of irrigated land<sup>44</sup>,  
352 which ranges from 1900 to 2005, and has been already used in other studies<sup>13,14,24</sup>. The soil  
353 attributes were based on the European Soil Database Derived data (ESDD)<sup>21,29,30</sup> and the land  
354 cover on the CORINE land cover dataset<sup>26</sup>. Both are widely used products which have been  
355 used in previous LSH datasets covering Europe<sup>7,8</sup>.

## 356 Data Records

357 The current version of the EStreams dataset and catalogue (v0.2) is stored at a Zenodo  
358 repository<sup>47</sup> at <https://doi.org/10.5281/zenodo.11609396>. The repository is organized into  
359 the following subfolders:

- 360 • **streamflow\_gauges**: Contains two csv-files. One includes all the metadata associated  
361 with each of the 17,130 streamflow gauging stations such as location, river name,  
362 catchment area, and gauge elevation. The other file is the streamflow catalogue  
363 containing all the data provider information, further described in the following  
364 section.
- 365 • **shapefiles**: Contains two shapefiles. One shapefile includes the derived catchment  
366 boundaries associated with each streamflow gauge, and the other shapefile marks the  
367 location of the streamflow gauges. Both files are referenced in WGS 84.
- 368 • **streamflow\_indices**: Contains one sub-folder per time resolution (weekly, monthly,  
369 seasonal and yearly) with a csv-file per computed index. The rows of each csv-file  
370 represent the time, and the columns represent the catchment.
- 371 • **meteorology**: Contains one csv-file per catchment (17,130 in total), each containing  
372 all the daily aggregated meteorological forcing records for that catchment (as detailed  
373 in **Table 6**). The rows of each csv-file represent the time, and the columns represent  
374 each of the 9 meteorological variables.
- 375 • **attributes**: Contains two sub folders. The **static\_attributes** subfolder contains one csv-  
376 file per attribute group (i.e., topography, soils, geology, hydrology, vegetation and  
377 landcover) encompassing all the attributes shown in **Table 7**. The rows of the csv-file  
378 represent the gauging stations, and the columns represent the attribute variable. The  
379 **temporal\_attributes** subfolder includes all the monthly or annual landscape attributes  
380 shown in **Table 8**. The csv-files in this subfolder are organized by gauging stations  
381 (rows), and attribute variables (columns), or as time series (each column represents  
382 one gauging station, and each row represents one date).

- 383
- 384
- 385
- 386
- 387
- 388
- **hydroclimatic\_signatures:** Contains one csv-file with all computed hydro-climatic signatures for all catchments. The rows of each csv-file represent the streamflow gauging station, and the columns represent each of the 25 derived signatures.
  - **appendix:** Contains three txt-files. One file provides descriptions of the lithological classes' labels, another describes the landcover classes' labels, and the third file includes licenses and data providers.

### 389 **Streamflow data catalogue**

390 An important component of EStreams is the streamflow catalogue, which provides complete  
391 guidance on how to retrieve the raw streamflow data used in this study to compute the  
392 streamflow statistics. **Table 9** provides an overview and description of the attribute fields  
393 included in the catalogue.

394 Particularly, the field **license\_redistribution** specifies the data redistribution policy of the  
395 data provider. In cases where this information is unavailable, users are advised to proceed  
396 with caution regarding any redistribution or specific use of the data, and to contact the data  
397 provider directly. The catalogue also includes various links to individual data providers,  
398 covering the website, the license source, streamflow and gauges metadata. Up to four  
399 different links are provided because the websites for downloading the streamflow time series  
400 may differ from those for gauge metadata.

401 The Zenodo repository<sup>47</sup> (<https://doi.org/10.5281/zenodo.11609396>) supports  
402 versioning, which ensures reproducibility, benchmarking, and the extensibility of the dataset  
403 as new stations or time periods are added.

404 Additionally, Jupyter Notebook demonstrations are available at the GitHub repository<sup>48</sup>  
405 (<https://doi.org/10.5281/zenodo.11654567>) showing not only how to use the catalogue but  
406 also allowing to directly retrieve and pre-process each of the daily records currently included  
407 in EStreams. The repository is linked to a GitHub page, enabling users to track potential  
408 changes in data providers, websites, and propose updates. This collaborative approach can  
409 lead to new releases of the catalogue, ensuring EStreams remains an updated and dynamic  
410 resource.

### 411 **Gauges layer**

412 A comprehensive overview of the gauges' attributes and metadata included in this dataset is  
413 presented in **Table 10**. These attributes are designed to offer users complete guidance on data  
414 availability before downloading, thereby optimizing the data collection process. The attributes  
415 include the gauges names and location, data provider, topographic information, temporal data  
416 availability, quality and reliability descriptors, and nested catchments & flow order attributes.  
417 These attributes ensure that users have detailed information to facilitate the efficient retrieval  
418 and application of the streamflow data in various hydrological analyses.

### 419 **Catchments layer**

420 The delineated boundary of each catchment is stored in the catchment layer. This layer  
421 includes the **basin\_id** field, which is also used for the gauges, allowing a link between the two  
422 datasets. Additionally, the catchment layer also has the fields **gauge\_id**, **gauge\_country** (here  
423 named **country**), **area\_official** (here named **area\_offic**), **area\_estreams** (here named  
424 **area\_estre**), **area\_flag**, **area\_rel**, **start\_date**, **end\_date**, **gauge\_flag**, **gauges\_upstream** (here  
425 named **upstream**) and **watershed\_group** (here named **group**), which were already described  
426 in **Table 10**. Note that **area\_official**, **area\_estreams**, **gauge\_country**, **gauges\_upstream** and  
427 **watershed\_group** had their names reduced due to storage limitations in the shape files. These  
428 fields ensure consistency between the catchment and gauge datasets, facilitating seamless  
429 integration and analysis.

## 430 Technical Validation

### 431 Duplicate stations

432 This work provides, alongside the gauges' metadata, information on potential candidates for  
433 duplication. This information is useful for users aiming to have a consistent dataset for their  
434 hydrological analysis. The results indicate that a total of 885 gauges are identified as potential  
435 duplicates, representing about 5% of the total. This means that more than 16,600 gauges in  
436 the dataset may be seen as unique gauging stations. The duplicates are divided into two types:  
437 gauges duplicated with other gauges within the same provider and gauges duplicated with  
438 other gauges within different providers.

439 These first types of duplicates often occur when gauges are discontinued and later  
440 reactivated as new stations, usually resulting in stations with non-overlapping time records  
441 but located at the same point. These cases are primarily found in France (449) and Finland  
442 (160). For example, stations FR001479 (1969-1999), FR001477 (1993-1999) and FR001478  
443 (2015-2023) are flagged as duplicate suspects among each other.

444 Additionally, 163 gauges are identified as duplicates across different data providers.  
445 These typically represent gauging stations located at the boundaries between countries and  
446 are mainly found in Austria (33), Switzerland (36) and Czech Republic (51). Interestingly,  
447 FR004543 is the only gauge identified as duplicate both within the same provider (FR002217)  
448 and across different providers (CH000268).

### 449 Basin delineation validation

450 In this part of the study, we used the dataset provided by LamaH-CE<sup>8</sup> for Austria, which  
451 includes both catchment boundaries and their respective officially reported areas. These were  
452 compared to the boundaries delineated using the methodology adopted in this work.

453 **Figure 5a** shows a scatter plot comparing the areas reported in LamaH-CE and those  
454 derived in EStreams. As expected, the scatter between the computed and reported areas is  
455 larger for smaller catchments. **Figure 5b** presents a histogram with the distribution of the  
456 relative absolute area difference  $|A_{rel}|$  between the two areas (in %). Out of the total of  
457 599 Austrian catchments, 539 had a  $|A_{rel}|$  below 10%. This indicates that roughly 90% of the  
458 catchments were accurately delineated during the automatic part of the delineation process.

459 However, if we consider only catchments with areas above 100 km<sup>2</sup> the number of  
460 catchments with  $|A_{rel}|$  above 10% drops from 60 to only 21. After visual inspection, we  
461 concluded that the main cause of these discrepancies was associated either to the difficulties  
462 in the delineation of relatively small catchments, below 100 km<sup>2</sup>, or to small discrepancies  
463 between the streamflow gauge location in terms of the MERIT-Hydro network.

464 **Figure 5c-d** illustrate an example of the catchment delineation workflow for  
465 catchment AT000009. This catchment has an  $A_{official}$  of 1281.0 km<sup>2</sup>. Initially,  $A_{EStream}$  derived an  
466 area of 4680.0 km<sup>2</sup>, which accounts for a  $A_{rel}$  of +265.0%. Upon visual inspection, we realized  
467 that the inconsistency was due to the inaccurate location of the streamflow gauge in relation  
468 to the MERIT-Hydro River network (**Figure 5c**). Since the outlet was not within the river  
469 network, the "delineator" python module used automatically moved it to the closest river  
470 network intersection, which had a much higher drainage area. After manually adjusting the  
471 streamflow gauge location, the delineation resulted in an area of 1,300.0 km<sup>2</sup>, an  $A_{rel}$  of only  
472 +1.5% (**Figure 5d**).

### 473 E-OBS assessment

#### 474 Spatial coverage

475 EStreams used E-OBS to derive the catchment aggregated time series of meteorological  
476 variables. However, the number of stations used to produce the gridded dataset varies  
477 significantly from country to country. Here we provide a brief overview of the station densities

478 used to derive the precipitation time series provided in E-OBS within each catchment. We  
479 present this analysis only for precipitation since it is considered the most important forcing  
480 input in hydrological studies and gives already a significant overview of the E-OBS network. To  
481 ensure a fair comparison, we considered a buffer of 10 km for the catchment boundaries and  
482 considered any station within this range to compute the number of stations.

483 **Figure 6a** illustrates the spatial distribution of the stations, revealing a large spatial  
484 variability in station density. Central and North Europe exhibit the highest density, with  
485 Germany and Poland taking leading in station density, while the density decreases significantly  
486 towards South and East.

487 **Figure 6b** presents the histogram of the station density per catchment included in  
488 EStreams. The x-axis is resampled to stations per 100 km<sup>2</sup> to facilitate visualization, with the  
489 threshold of less than one station per 100 km<sup>2</sup> marked in red. A total of 9,840 catchments have  
490 at least one precipitation gauge per 100 km<sup>2</sup>. This represents, a median of 1.2 stations per 100  
491 km<sup>2</sup>. Considering absolute terms, we found a total of 14,153 gauges with at least one  
492 precipitation station within their boundaries.

493 This information enables users to be aware of the highly variable quality of the  
494 provided E-OBS data and make informed decisions, especially considering the critical role of  
495 accurate precipitation data in many hydrological applications. Like streamflow data, national  
496 providers typically offer much higher resolution precipitation data compared to global  
497 databases<sup>49</sup>. While retrieving this information was beyond the scope of this study, users may  
498 choose to leverage such local data sources, particularly in regions where station density is  
499 notably low, such as in the South, East, and West of Europe.

## 500 **Validation of meteorological forcing**

501 We further validated the aggregated precipitation derived from E-OBS comparing it to the  
502 reported time series available at CAMELS-CH<sup>7</sup> and CAMELS-GB<sup>6</sup>. Given that the aggregation of  
503 the forcing variables used E-OBS gridded data with a resolution of 0.25 degrees, we opted to  
504 include only catchments with areas above 100 km<sup>2</sup> in the comparison.

505 **Figure 7a** shows a scatter plot illustrating the daily precipitation from E-OBS and  
506 CAMELS. CAMELS-GB is represented in blue and CAMELS-CH in orange. A notable  
507 correspondence between the two sources is observable, with correlation coefficients of 0.89  
508 for GB and 0.94 for CH. Generally, the scatter is lower in catchments with higher daily mean  
509 precipitation and an underestimation from E-OBS compared to the two sources is evident.

510 **Figure 7b** shows the distribution of the correlation coefficients between each daily  
511 time series of E-OBS and CAMELS. Again, it is possible to observe that most of the catchments  
512 presented a correlation above 0.8, indicating some agreement between the two precipitation  
513 sources. Overall, CAMELS-CH demonstrates higher correlation coefficients than CAMELS-GB.  
514 Despite this comparison only encompassing two different regions within the large span  
515 covered by EStreams, it was conducted using two independent sources. Hence, this analysis  
516 suggests that E-OBS, at least in countries where the station density is relatively high, provides  
517 a broadly consistent starting point for representing precipitation time series.

## 518 **Usage Notes**

519 **Aggregated data:** The original data used to aggregate the catchment attributes such as  
520 climate, geology, hydrology, land use and land cover, soil types and vegetation characteristics  
521 have all continental or global resolution. It should be kept in mind that such resolution is rather  
522 coarse compared to local information usually available at the national scales, but seldom easily  
523 accessible. We therefore recommend that users acknowledge these potential limitations  
524 when using the landscape aggregated data. Additionally, we recommend users to also  
525 reference the original sources when using the aggregated data provided in EStreams.

526 **Streamflow catalogue:** We recognize that potential retrospective check and updates of  
527 streamflow time series by the data providers may alter the information of the gauges  
528 metadata provided here. We also acknowledge that potential changes in the data providers'  
529 platforms may alter the available links in the catalogue. Therefore, we invite the users to  
530 access the latest version of the catalogue and dataset on the Zenodo repository<sup>47</sup> page for  
531 potential updates.

532 **Instructions for Python:** We kindly request that future users of the EStreams' codes read and  
533 follow carefully the instructions provided in the scripts. Specifically, (i) use the specified  
534 version of the Python modules (requirements.txt); (ii) clone the repository locally and keep all  
535 the original folders' names; (iii) place the original data in their specified folder and with their  
536 expected filename and version; (iv) follow the pre-defined specified order of run for the  
537 available scripts (when necessary). Be aware that the potential main source of problems when  
538 running the scripts might be caused by not following these guidelines.

### 539 **Code Availability**

540 The current version of the code used to produce the EStreams dataset and catalogue (v0.2.0)  
541 is available at a Zenodo repository<sup>49</sup> at <https://doi.org/10.5281/zenodo.11654567>. For the  
542 latest version of the code, users are invited to visit the project GitHub repository at  
543 <https://github.com/thiagovmdon/EStreams>. The scripts are organized to enable users to  
544 follow a logical sequence during code usage. All data processing scripts are written in Python,  
545 while some data retrieval tasks are performed using JavaScript for the Google Earth Engine  
546 (GEE) platform. Although all scripts are executable, users must download and preprocess the  
547 original data due to redistribution licenses. Detailed instructions regarding the version used,  
548 data retrieval, and any required preprocessing are provided within the respective scripts.

### 549 **References**

- 550  
551  
552  
553  
554  
555  
556  
557  
558  
559  
560  
561  
562  
563  
564  
565  
566  
567  
568  
569  
570  
571  
572  
573  
574  
575  
576  
577  
578  
579
1. Addor, N., Newman, A. J., Mizukami, N. & Clark, M. P. The CAMELS data set: Catchment attributes and meteorology for large-sample studies. *Hydrol Earth Syst Sci* **21**, 5293–5313 (2017).
  2. Coxon, G. *et al.* CAMELS-GB: hydrometeorological time series and landscape attributes for 671 catchments in Great Britain. *Earth Syst Sci Data* **12**, 2459–2483 (2020).
  3. Kratzert, F. *et al.* Caravan - A global community dataset for large-sample hydrology. *Scientific Data* **2023 10:1** **10**, 1–11 (2023).
  4. Fowler, K. J. A., Acharya, S. C., Addor, N., Chou, C. & Peel, M. C. CAMELS-AUS: Hydrometeorological time series and landscape attributes for 222 catchments in Australia. *Earth Syst Sci Data* **13**, 3847–3867 (2021).
  5. Chagas, V. B. P. *et al.* CAMELS-BR: Hydrometeorological time series and landscape attributes for 897 catchments in Brazil. *Earth Syst Sci Data* **12**, 2075–2096 (2020).
  6. Alvarez-Garreton, C. *et al.* The CAMELS-CL dataset: Catchment attributes and meteorology for large sample studies-Chile dataset. *Hydrol Earth Syst Sci* **22**, 5817–5846 (2018).
  7. Höge, M. *et al.* CAMELS-CH: hydro-meteorological time series and landscape attributes for 331 catchments in hydrologic Switzerland. *Earth Syst Sci Data* **15**, 5755–5784 (2023).
  8. Klingler, C., Schulz, K. & Herrnegger, M. LamaH-CE: LARge-SaMple DAta for Hydrology and Environmental Sciences for Central Europe. *Earth Syst Sci Data* **13**, 4529–4565 (2021).
  9. Arsenault, R. *et al.* A comprehensive, multisource database for hydrometeorological modeling of 14,425 North American watersheds. *Scientific Data* **2020 7:1** **7**, 1–12 (2020).
  10. Hao, Z. *et al.* CCAM: China Catchment Attributes and Meteorology dataset. *Earth Syst Sci Data* **13**, 5591–5616 (2021).
  11. Marti, B. *et al.* CA-discharge: Geo-Located Discharge Time Series for Mountainous Rivers in Central Asia. *Scientific Data* **2023 10:1** **10**, 1–21 (2023).
  12. Helgason, H. B. & Nijssen, B. LamaH-Ice: LARge-SaMple DAta for Hydrology and Environmental Sciences for Iceland, CUAHSI HydroShare (last access: 01 May 2024). *2023* <https://www.hydroshare.org/resource/86117a5f36cc4b7c90a5d54e18161c91/>.
  13. Do, H. X., Gudmundsson, L., Leonard, M. & Westra, S. The Global Streamflow Indices and Metadata Archive (GSIM)-Part 1: The production of a daily streamflow archive and metadata. *Earth Syst Sci Data* **10**, 765–785 (2018).

- 580 14. Gudmundsson, L., Do, H. X., Leonard, M. & Westra, S. The Global Streamflow Indices and Metadata  
581 Archive (GSIM)-Part 2: Quality control, time-series indices and homogeneity assessment. *Earth Syst Sci*  
582 *Data* **10**, 787–804 (2018).
- 583 15. Chen, X., Jiang, L., Luo, Y. & Liu, J. A global streamflow indices time series dataset for large-sample  
584 hydrological analyses on streamflow regime (until 2022). *Earth Syst Sci Data* **15**, 4463–4479 (2023).
- 585 16. GRDC. Global Runoff Data Center: River discharge data. Federal Institute of Hydrology, 56068 Koblenz,  
586 Germany. <https://www.bafg.de/GRDC> (last access: 01 May 2024).
- 587 17. Färber, C. *et al.* GRDC-Caravan: extending the original dataset with data from the Global Runoff Data  
588 Centre (0.1) [Data set]. *Zenodo* <https://zenodo.org/records/8425587> (2023)  
589 doi:10.5281/ZENODO.8425587.
- 590 18. Hersbach, H. *et al.* The ERA5 global reanalysis. *Quarterly Journal of the Royal Meteorological Society* **146**,  
591 1999–2049 (2020).
- 592 19. Cornes, R. C., van der Schrier, G., van den Besselaar, E. J. M. & Jones, P. D. An Ensemble Version of the E-  
593 OBS Temperature and Precipitation Data Sets. *Journal of Geophysical Research: Atmospheres* **123**, 9391–  
594 9409 (2018).
- 595 20. Hartmann, J., Moosdorf, N., Hartmann, J. & Moosdorf, N. The new global lithological map database  
596 GLiM: A representation of rock properties at the Earth surface. *Geochemistry, Geophysics, Geosystems*  
597 **13**, 12004 (2012).
- 598 21. Pelletier, J. D. *et al.* A gridded global data set of soil, intact regolith, and sedimentary deposit thicknesses  
599 for regional and global land surface modeling. *J Adv Model Earth Syst* **8**, 41–65 (2016).
- 600 22. Yamazaki, D. *et al.* MERIT Hydro: A High-Resolution Global Hydrography Map Based on Latest  
601 Topography Dataset. *Water Resour Res* **55**, 5053–5073 (2019).
- 602 23. Wang, J. *et al.* GeoDAR: georeferenced global dams and reservoirs dataset for bridging attributes and  
603 geolocations. *Earth Syst Sci Data* **14**, 1869–1899 (2022).
- 604 24. Linke, S. *et al.* Global hydro-environmental sub-basin and river reach characteristics at high spatial  
605 resolution. *Scientific Data* **2019** 6:1 **6**, 1–15 (2019).
- 606 25. Yamazaki, D. *et al.* A high-accuracy map of global terrain elevations. *Geophys Res Lett* **44**, 5844–5853  
607 (2017).
- 608 26. CORINE: CORINE Land Cover — Copernicus Land Monitoring Service. *European Environment Agency*  
609 *[data set]*, Copenhagen, Denmark <https://land.copernicus.eu/en/products/corine-land-cover>.
- 610 27. Siebert, S. *et al.* A global data set of the extent of irrigated land from 1900 to 2005. *Hydrol Earth Syst Sci*  
611 **19**, 1521–1545 (2015).
- 612 28. Hall, D. K. & Riggs, G. A. MODIS/Terra Snow Cover Daily L3 Global 500m SIN Grid, Version 61 [Data Set].  
613 *NASA National Snow and Ice Data Center Distributed Active Archive Center*. vol. 21  
614 <https://doi.org/10.5067/MODIS/MOD10A1.061> (2021).
- 615 29. Hiederer, R. *Mapping Soil Typologies – Spatial Decision Support Applied to European Soil Database*.  
616 <https://doi.org/10.2788/87286> (2013).
- 617 30. Hiederer, R. *Mapping Soil Properties for Europe – Spatial Representation of Soil Database Attributes*.  
618 <https://data.europa.eu/doi/10.2788/94128> (2013).
- 619 31. ESDD. *European Soil Database Derived Data*. [https://Esdac.Jrc.Ec.Europa.Eu/Content/European-Soil-](https://Esdac.Jrc.Ec.Europa.Eu/Content/European-Soil-Database-Derived-Data)  
620 *Database-Derived-Data* (Last Access: 23 Nov 2023).
- 621 32. Didan, K. MODIS/Terra Vegetation Indices 16-Day L3 Global 500m SIN Grid V061 [Data set]. *ASA EOSDIS*  
622 *Land Processes Distributed Active Archive Center* <https://doi.org/10.5067/MODIS/MOD13A1.061> (2021).
- 623 33. Myneni, R., Knyazikhin, Y. & Park, T. MODIS/Terra Leaf Area Index/FPAR 8-Day L4 Global 500m SIN Grid  
624 V061 [Data set]. *NASA EOSDIS Land Processes Distributed Active Archive Center*  
625 <https://doi.org/10.5067/MODIS/MOD15A2H.061> (2021).
- 626 34. Christen, P. Data matching: Concepts and techniques for record linkage, entity resolution, and duplicate  
627 detection. *Data Matching: Concepts and Techniques for Record Linkage, Entity Resolution, and Duplicate*  
628 *Detection* 1–270 (2012) doi:10.1007/978-3-642-31164-2/COVER.
- 629 35. Trambly, Y. *et al.* ADHI: The African Database of Hydrometric Indices (1950–2018). *Earth Syst Sci Data*  
630 **13**, 1547–1560 (2021).
- 631 36. Crochemore, L. *et al.* Lessons learnt from checking the quality of openly accessible river flow data  
632 worldwide. *Hydrological Sciences Journal* **65**, 699–711 (2020).
- 633 37. Heberger, M. delineator.py: fast, accurate global watershed delineation using hybrid vector- and raster-  
634 based methods. 2022 <https://doi.org/10.5281/zenodo.7314287> doi:10.5281/ZENODO.7314287.
- 635 38. COPERNICUS Land Monitoring Service. EU-Hydro. <https://land.copernicus.eu/imagery-in-situ/eu-hydro>  
636 (last access: 18 Aug 2023). 2019.
- 637 39. Dal Molin, M. dalmo1991/HydroAnalysis: v1.0.0 (1.0.0). *Zenodo*.  
638 <https://doi.org/10.5281/zenodo.5716016> (2021) doi:10.5281/ZENODO.5716016.
- 639 40. Wunsch, A. *et al.* Karst spring discharge modeling based on deep learning using spatially distributed input  
640 data. *Hydrol Earth Syst Sci* **26**, 2405–2430 (2022).
- 641 41. Rojas, R., Feyen, L., Dosio, A. & Bavera, D. Improving pan-European hydrological simulation of extreme  
642 events through statistical bias correction of RCM-driven climate simulations. *Hydrol Earth Syst Sci* **15**,  
643 2599–2620 (2011).

- 644 42. Becker, A. *et al.* A description of the global land-surface precipitation data products of the Global  
645 Precipitation Climatology Centre with sample applications including centennial (trend) analysis from  
646 1901-present. *Earth Syst Sci Data* **5**, 71–99 (2013).
- 647 43. Bandhauer, M. *et al.* Evaluation of daily precipitation analyses in E-OBS (v19.0e) and ERA5 by comparison  
648 to regional high-resolution datasets in European regions. *International Journal of Climatology* **42**, 727–  
649 747 (2022).
- 650 44. Hargreaves, G. H. & Samani, Z. A. Estimating potential evapotranspiration. *Journal of Irrigation and*  
651 *Drainage Engineering* **108**, 223–230 (1982).
- 652 45. Vremec, M. & Collenteur, R. PyEt-a Python package to estimate potential and reference  
653 evapotranspiration 1.1.0. in *EGU General Assembly Conference Abstracts* (2021).
- 654 46. Messenger, M. L., Lehner, B., Grill, G., Nedeva, I. & Schmitt, O. Estimating the volume and age of water  
655 stored in global lakes using a geo-statistical approach. *Nature Communications* **2016 7:1 7**, 1–11 (2016).
- 656 47. do Nascimento, T. V. M. , *et al.* EStreams: An Integrated Dataset and Catalogue of Streamflow, Hydro-  
657 Climatic Variables and Landscape Descriptors for Europe (0.2) [Data set]. *Zenodo* (2024)  
658 doi:<https://doi.org/10.5281/zenodo.11609396>.
- 659 48. do Nascimento, T. V. M. , *et al.* EStreams: An Integrated Dataset and Catalogue of Streamflow, Hydro-  
660 Climatic Variables and Landscape Descriptors for Europe (v.0.2.0) [Code]. *Zenodo*  
661 <https://doi.org/10.5281/zenodo.11654567> (2024).
- 662 49. Clerc-Schwarzenbach, F. M. *et al.* HESS Opinions: A few camels or a whole caravan? *EGUsphere [preprint]*  
663 (2024) doi:<https://doi.org/10.5194/egusphere-2024-864>.
- 664 50. Jordahl, K. *et al.* geopandas/geopandas: v0.8.1 <https://zenodo.org/doi/10.5281/zenodo.2585848>.  
665 (2020).
- 666 51. BML. Federal Ministry of Agriculture, Forestry, Regions and Water Management: WebGIS-Applikation  
667 eHYD, Wien, Austria, <https://ehyd.gv.at> (last access: 05 May 2023).
- 668 52. FHMZBIH. Federalni hidrometeorološki zavod: Početna: idrologija: hidrološki godišnjaci, Bosnia.  
669 <https://www.fhmzbih.gov.ba/latinica/HIDRO/godisnjaci.php> (last access: 29 June 2023).
- 670 53. VW. Vlaanderen waterinfo, Belgium. <https://www.waterinfo.be/kaartencatalogus?KL=en> (last access: 07  
671 Dec 2023).
- 672 54. SPW. Service public de Wallonie: L'hydrométrie en Wallonie: Observations: Debit, Belgium.  
673 <https://hydrometrie.wallonie.be/home/observations/debit.html?mode=announcement> (last access: 07  
674 Dec 2023).
- 675 55. BAFU. Federal Office for the Environment, Switzerland. <https://www.bafu.admin.ch/bafu/en/home.html>  
676 (last access: 15 May 2023).
- 677 56. CHMI. Czech Hydrometeorological Institute: ISVS - Evidence množství povrchových vod.  
678 [https://isvs.chmi.cz/ords/f?p=11002:HOME:5026647009329::: \(last access: 10 Jul 2023\).](https://isvs.chmi.cz/ords/f?p=11002:HOME:5026647009329:::)
- 679 57. LHW. Landesbetrieb für Hochwasserschutz und Wasserwirtschaft Sachsen-Anhalt, [https://gld.lhw-  
680 sachsen-anhalt.de/](https://gld.lhw-sachsen-anhalt.de/) (last access: 12 Dec 2023).
- 681 58. ASOEAG. Saxon State Office for Environment, Agriculture and Geology: Datenportal für Umweltdaten  
682 Sachsen (iDA),  
683 [https://www.umwelt.sachsen.de/umwelt/infosysteme/ida/processingChain?conditionValuesSetHash=0  
684 A8BBED&selector=ROOT.Thema%20Wasser.Oberirdische%20Gew%C3%A4sser.Pegel.Wasserstand%20u  
685 nd%20Durchfluss.OWMN%3Aowmn\\_menge\\_tagesmittelwerte\\_v2.sel&sourceOrderAsc=false&columns=  
686 9dfa2224-c924-4328-9805-1d34cd748026&offset=0&limit=2147483647&executionConfirmed=false](https://www.umwelt.sachsen.de/umwelt/infosysteme/ida/processingChain?conditionValuesSetHash=0A8BBED&selector=ROOT.Thema%20Wasser.Oberirdische%20Gew%C3%A4sser.Pegel.Wasserstand%20und%20Durchfluss.OWMN%3Aowmn_menge_tagesmittelwerte_v2.sel&sourceOrderAsc=false&columns=9dfa2224-c924-4328-9805-1d34cd748026&offset=0&limit=2147483647&executionConfirmed=false) (last  
687 access: 12 Dec 2023).
- 688 59. Umweltportal. Schleswig-Holstein, Germany. [https://umweltportal.schleswig-  
689 holstein.de/kartendienste?lang=de&topic=thessd&bgLayer=sgx\\_geodatenzentrum\\_de\\_de\\_basemapde\\_  
690 web\\_raster\\_grau\\_DE\\_EPSG\\_25832\\_ADV&E=567583.34&N=5998716.15&zoom=4&layers=262b5c716ef5  
691 358fc1ac1e34afd45915](https://umweltportal.schleswig-holstein.de/kartendienste?lang=de&topic=thessd&bgLayer=sgx_geodatenzentrum_de_de_basemapde_web_raster_grau_DE_EPSG_25832_ADV&E=567583.34&N=5998716.15&zoom=4&layers=262b5c716ef5358fc1ac1e34afd45915) (last access: 12 Dec 2023).
- 692 60. ELWAS-WEB. Ministerium für Umwelt, Naturschutz und Verkehr des Landes Nordrhein-Westfalen,  
693 [https://www.elwasweb.nrw.de/elwas-web/data-  
694 objekt;jsessionid=DADDD7196B89E206917D18793294E375;jsessionid=F76CC7CC8ECFBA5F518ECD241AF  
695 0BA78?art=Pegel](https://www.elwasweb.nrw.de/elwas-web/data-objekt;jsessionid=DADDD7196B89E206917D18793294E375;jsessionid=F76CC7CC8ECFBA5F518ECD241AF0BA78?art=Pegel) (last access: 12 Dec 2023).
- 696 61. NLWKN. Niedersächsischer Landesbetrieb für Wasserwirtschaft, Küsten- und Naturschutz,  
697 [http://www.wasserdaten.niedersachsen.de/cadenza/pages/selector/index.xhtml;jsessionid=1E0F808EF5  
698 8258C4EE5C777447D1ED4A](http://www.wasserdaten.niedersachsen.de/cadenza/pages/selector/index.xhtml;jsessionid=1E0F808EF58258C4EE5C777447D1ED4A) (last access: 12 Dec 2023).
- 699 62. HLNUG. Hessisches Landesamt für Naturschutz, Umwelt und Geologie.  
700 [https://www.hlnug.de/static/pegel/wikiweb3/webpublic/#/overview/Wasserstand?mode=table&filter=  
701 %7B%7D](https://www.hlnug.de/static/pegel/wikiweb3/webpublic/#/overview/Wasserstand?mode=table&filter=%7B%7D) (last access: 12 Dec 2023).
- 702 63. GKD. Bavarian State Office for the Environment – Hydrographic Service, Munich, Germany  
703 <https://www.gkd.bayern.de/en/rivers/discharge/tables> (last access: 12 Dec 2023).
- 704 64. LUBW. State Agency for the Environment Baden-Württemberg – Hydrographic Service, Karlsruhe,  
705 Germany. <https://udo.lubw.baden-wuerttemberg.de/public/> (last access: 12 Dec 2023).
- 706 65. WB. Das Wasserportal Berlin: <https://wasserportal.berlin.de/start.php> (last access: 12 Dec 2023).

- 707 66. LBAW. Land Brandenburg Auskunftsplattform Wasser. [https://apw.brandenburg.de/?th=owm\\_gkp/](https://apw.brandenburg.de/?th=owm_gkp/) (last  
708 access: 12 Dec 2023).
- 709 67. MKUEM. Ministerium für Klimaschutz, Umwelt, Energie und Mobilität: Rheinland-Pfalz, Germany.  
710 <https://wasserportal.rlp-umwelt.de> (data received: 13 Mar 2023).
- 711 68. LUBN. Landesamt für Umwelt, Bergbau und Naturschutz. Hochwasser Nachrichten Zentrale: Freistaat  
712 Thüringen. <https://hnz.thueringen.de> (data received: 13 Mar 2023).
- 713 69. BFG. Bundesanstalt für Gewässerkunde, Germany.  
714 [https://www.bafg.de/DE/Home/homepage\\_node.html](https://www.bafg.de/DE/Home/homepage_node.html) (data received: 13 Mar 2023).
- 715 70. ODA. Overfladevandsdatabasen: Aarhus University, Denmark. <https://odaforalle.au.dk/login.aspx> (last  
716 access: 17 Jul 2023).
- 717 71. CEDEX. Centro de Estudios y Experimentación de Obras Publicas: Anuario de aforos 2019-2020, Spain.  
718 <https://ceh.cedex.es/anuarioaforos/demarcaciones.asp> (last access: 12 Apr 2023).
- 719 72. FEI. Finish Environmental Institute, Finland. <https://www.p2ymparisto.fi/scripts/kirjautu.asp> (last access:  
720 10 Jul 2023).
- 721 73. BanqueHydro. Hydro Portail, France. <https://www.hydro.eaufrance.fr/> (last access: 01 May 2024).
- 722 74. NRFA. National River Flow Archive API, United Kingdom. <https://nrfaapps.ceh.ac.uk/nrfa/nrfa-api.html>  
723 (last access: 07 Jul 2023).
- 724 75. OHIN. Open Hydrosystem Information Network, Greece. <https://openhi.net/en/> (last access: 12 Oct  
725 2023).
- 726 76. HCRM. Institute of Marine Biological Resources and Inland Waters, Greece. [https://hydro-  
727 stations.hcmr.gr/%cf%80%ce%b1%cf%81%ce%bf%cf%87%ce%ae-  
728 %cf%80%ce%bf%cf%84%ce%b1%ce%bc%cf%8e%ce%bd/](https://hydro-stations.hcmr.gr/%cf%80%ce%b1%cf%81%ce%bf%cf%87%ce%ae-%cf%80%ce%bf%cf%84%ce%b1%ce%bc%cf%8e%ce%bd/) (last access: 12 Oct 2023).
- 729 77. DHZ. Croatian Meteorological and Hydrological Service. <https://hidro.dhz.hr/> (last access: 01 May 2024).
- 730 78. OVf. General Directorate of Water Management. <https://ovf.hu/kozerdeku/adatigenyles> (data received:  
731 18 Aug 2023).
- 732 79. EPA. Environmental Protection Agency, Ireland. <https://epawebapp.epa.ie/hydronet/#Flow> (last access:  
733 27 Jun 2023).
- 734 80. OPW. Office of Public Works, Ireland. <https://waterlevel.ie/hydro-data> (last access: 27 Jun 2023).
- 735 81. ISPRA. Institute Superiore per la Protezione e la Ricerca Ambientale, Italy.  
736 <http://www.hiscentral.isprambiente.gov.it/hiscentral/hydromap.aspx?map=obsclient>, (last access: 30  
737 December 2023).
- 738 82. APC Abruzzo. Centro Funzionale e Ufficio Idrologia, Idrografico, Mareografico: Agenzia di Protezione  
739 Civile della Regione Abruzzo, Italy (data received: 02 August 2023).
- 740 83. CFRA Valle d'Aosta. Centro Funzionale Regione Autonoma Valle d'Aosta, Italy.  
741 [https://presidi2.regione.vda.it/str\\_dataview\\_download](https://presidi2.regione.vda.it/str_dataview_download) (last access: 19 May 2023).
- 742 84. ARPAE Emilia-Romagna. Agenzia Prevenzione Ambiente Energia - Emilia-Romagna, Italy.  
743 <https://simc.arpae.it/dext3r/> (last access: 04 Nov 2023).
- 744 85. ARPA Umbria. Agenzia Regionale per la Protezione dell Ambiente - Umbria, Italy.  
745 <https://annali.regione.umbria.it> (last access: 22 May 2023).
- 746 86. ARPA Sardegna. Agenzia Regionale per la Protezione dell Ambiente - Sardegna, Italy.  
747 <https://www.sardegnaambiente.it/index.php?xsl=611&s=21&v=9&c=93749&na=1&n=10> (last access: 30  
748 December 2023).
- 749 87. ARPA Lombardia. Agenzia Regionale per la Protezione dell Ambiente - Lombardia, Italy. (data received:  
750 17 Jun 2023).
- 751 88. ARPA Lombardia. Agenzia Regionale per la Protezione dell Ambiente - Lombardia, Italy.  
752 [https://idro.arpalombardia.it/manual/dati\\_storici.html](https://idro.arpalombardia.it/manual/dati_storici.html) (last access: 24 May 2023).
- 753 89. ARPA Toscana. Agenzia Regionale per la Protezione dell Ambiente - Toscana, Italy.  
754 <http://www.sir.toscana.it/consistenza-rete> (last access: 16 Jun 2023).
- 755 90. ARPA Piemonte. Agenzia Regionale per la Protezione dell Ambiente - Piemonte, Italy.  
756 [https://www.arpa.piemonte.it/rischi\\_naturali/snippets\\_arpa\\_graphs/map\\_meteoweb/?rete=  
757 stazione\\_meteorologica](https://www.arpa.piemonte.it/rischi_naturali/snippets_arpa_graphs/map_meteoweb/?rete=stazione_meteorologica) (last access: 22 May 2023).
- 758 91. ARPAL Liguria. Agenzia Regionale per la Protezione dell Ambiente - Liguria, Italy.  
759 <https://www.arpal.liguria.it> (data received: 08 Jun 2023).
- 760 92. ARPAV Veneto. Agenzia Regionale per la Prevenzione e Protezione Ambientale del Veneto, Italy.  
761 <https://www.arpa.veneto.it/> (data received: 30 Jun 2023).
- 762 93. SPRUD Trentino. Servizio Prevenzioni Rischi Ufficio Dighe - Trentino-Alto Adige Trento, Italy.  
763 <https://www.floods.it/public/DatiStorici.php> (last access: 24 May 2023).
- 764 94. NGGL. The National Geoportal of the Grand-Dutchy of Luxembourg. <https://map.geoportail.lu> (data  
765 received: 13 Mar 2023).
- 766 95. RWS. Rijkswaterstaat waterinfo, The Netherlands. <https://waterinfo.rws.nl/#/publiek/waterafvoer> (last  
767 access: 07 Dec 2023).
- 768 96. NVE. Norwegian Water Resources and Energy Directorate, Norway. <https://seriekart.nve.no> (last access:  
769 10 Jul 2023).

- 770 97. IMGW-PIB. Institute of Meteorology and Water Management - National Research Institute, Warszawa,  
771 Poland. <https://danepubliczne.imgw.pl/introduction> (last access: 30 Dec 2023).  
772 98. SNIRH. Sistema Nacional de Informação de Recursos Hídricos: Dados de Base, Portugal.  
773 <https://snirh.apambiente.pt/index.php?idMain=2&idItem=1> (last access: 01 May 2024).  
774 99. SMHI. Swedish Meteorological and Hydrological Institute, Sweden.  
775 [https://www.smhi.se/data/hydrologi/ladda-ner-hydrologiska-](https://www.smhi.se/data/hydrologi/ladda-ner-hydrologiska-observationer#param=waterdischargeDaily,stations=core)  
776 [observationer#param=waterdischargeDaily,stations=core](https://www.smhi.se/data/hydrologi/ladda-ner-hydrologiska-observationer#param=waterdischargeDaily,stations=core) (last access: 30 Dec 2023).  
777 100. ARSO. Agencija Republike Slovenije za Okolje, Ljubljana, Slovenia. <https://vode.arso.gov.si/hidarhiv/> (last  
778 access: 23 Jun 2023).  
779 101. Sankarasubramanian, A., Vogel, R. M. & Limbrunner, J. F. Climate elasticity of streamflow in the United  
780 States. *Water Resour Res* **37**, 1771–1781 (2001).  
781 102. Sawicz, K., Wagener, T., Sivapalan, M., Troch, P. A. & Carrillo, G. Catchment classification: Empirical  
782 analysis of hydrologic similarity based on catchment function in the eastern USA. *Hydrol Earth Syst Sci*  
783 **15**, 2895–2911 (2011).  
784 103. Ladson, A. R., Brown, R., Neal, B. & Nathan, R. A standard approach to baseflow separation using the  
785 Lyne and Hollick filter. *Australian Journal of Water Resources* **17**, 25–34 (2013).  
786 104. Schumm, S. A. Evolution of drainage systems and slopes in badlands at Perth Amboy, New Jersey. *GSA*  
787 *Bulletin* **67**, 597–646 (1956).  
788

## 789 **Acknowledgements**

790 This project was funded by a “Money Follows Cooperation” project (Project No.  
791 OCENW.M.21.230) between the Netherlands Organization for Scientific Research (NWO) and  
792 the Swiss National Science Foundation (SNSF). This work was further supported by the TU Delft  
793 Climate Action Research and Education seed funds. We would like to acknowledge all the data  
794 providers and contact people who somehow contributed to the construction of this dataset.  
795 In particular, we thank acknowledge specially the E-OBS dataset, the data providers in the  
796 ECA&D project (<https://www.ecad.eu>), the European Soil Database Derived data project  
797 (ESDAC) and the UK National River Flow Archive.

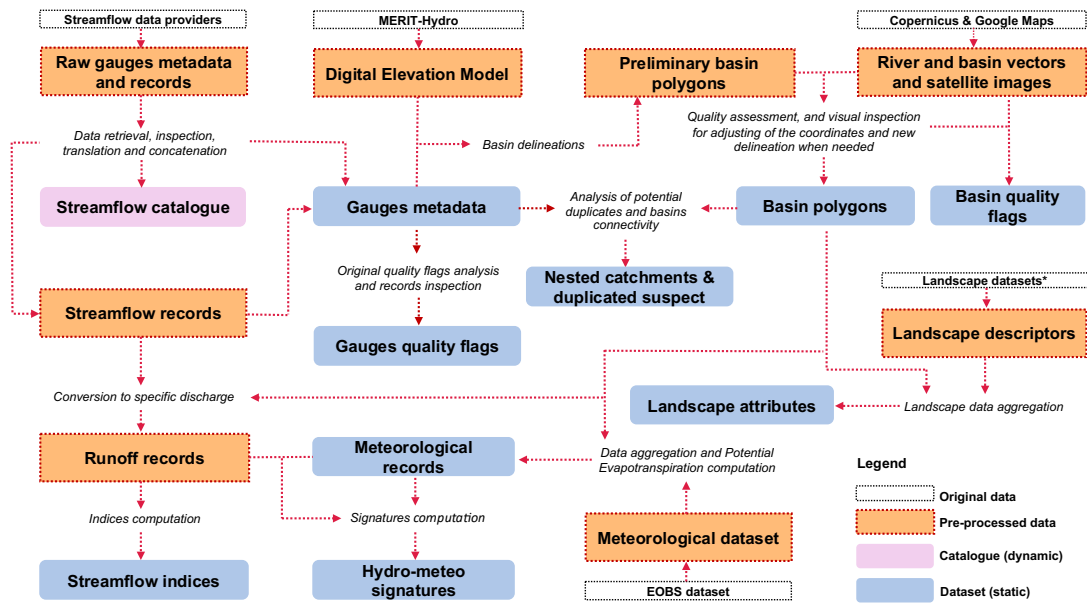
## 798 **Author contributions**

799 The co-authors T.N., J.R., R.E., M.H., J.S. M.Hr. and F.F. were involved in the development of  
800 the concept of this paper. T.N. and J.R. collected and pre-processed the data. M.C. provided  
801 guidance to some data providers in Eastern Europe. T.N. wrote the data aggregation and  
802 processing codes in Python and Google Earth Engine. T.N. and J.R. processed the catchment  
803 boundaries. T.N. wrote the first draft. M.Hr and F.F. retrieved the funding for the project. All  
804 co-authors participated in reviewing the manuscript.

## 805 **Competing interests**

806 The authors declare no competing interests.

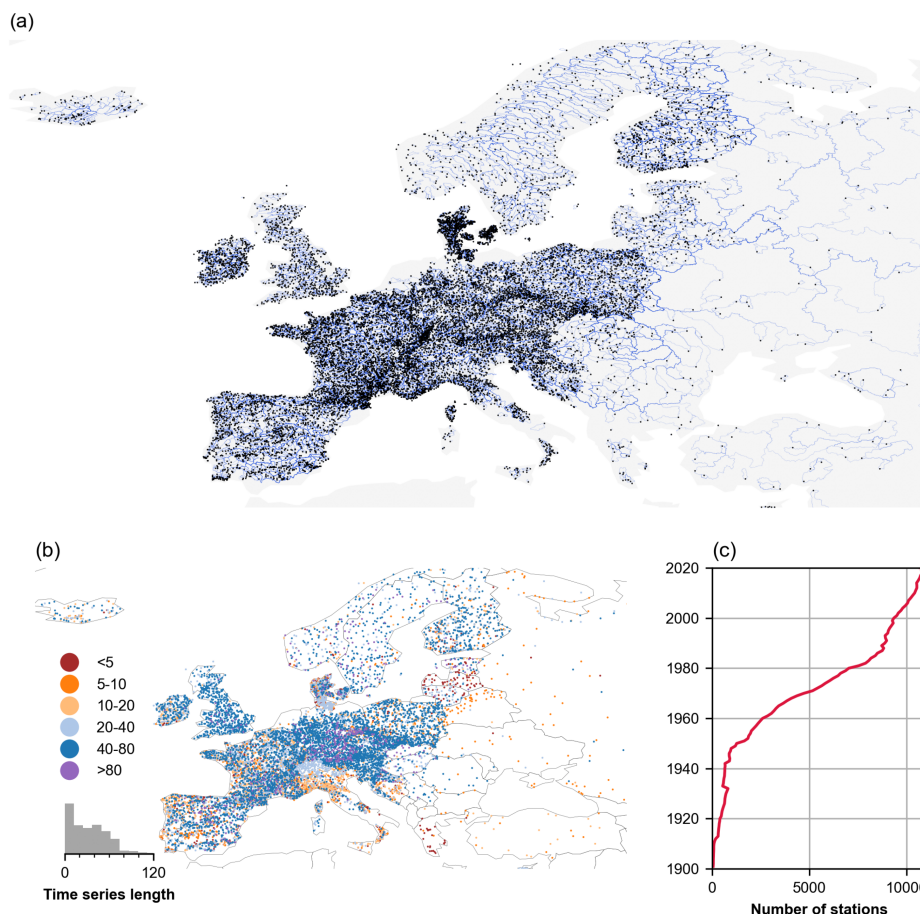
## 807 **Figures & Tables**



808  
809  
810  
811  
812  
813

**Figure 1.** Framework of the methodology adopted in EStreams for deriving the Streamflow Catalogue, and the Dataset. The boxes with dashed lines represent the original, and the intermediate (pre-processed) data used in EStreams. The outputs are shown in purple (catalogue) and blue (dataset).

\* The landscape datasets encompass topography, soils, geology, hydrology, vegetation and land cover.



814  
815  
816  
817

**Figure 2.** (a) Spatial distribution of the 17,130 streamflow gauges currently included in EStreams (in black dots) with their catchment boundaries in background (in blue) over Europe. (b) Spatial distribution of the streamflow with the colors representing the time series length in years. (c) Temporal evolution

818  
819

of station coverage. The plot shows the number of active stations in a given year, Although the curve accounts for dismissed stations, it still shows an increasing trend. Basemap from GeoPandas<sup>50</sup>.

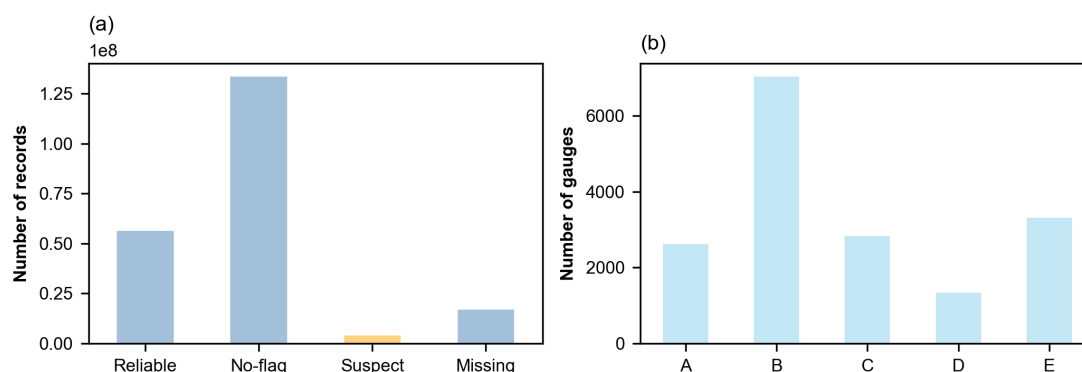
Country/region	Code	Stations	References
Austria	AT	582	BML <sup>51</sup>
Bosnia and H.	BA	91	GDRC <sup>16</sup> ; FHMZBIH <sup>52</sup>
Belgium	BE	230	VW <sup>53</sup> ; SPW <sup>54</sup>
Bulgaria	BG	8	GRDC <sup>16</sup>
Belarus	BY	51	GRDC <sup>16</sup>
Switzerland	CH	298	BAFU <sup>7,55</sup>
Cyprus	CY	14	GRDC <sup>16</sup>
Czechia	CZ	566	CHMI <sup>56</sup>
Germany	DE	2,093	LHW <sup>57</sup> ; ASOEAG <sup>58</sup> ; Umweltportal <sup>59</sup> ; ELWAS-WEB <sup>60</sup> ; NLWKN <sup>61</sup> ; HLNUG <sup>62</sup> ; GKD <sup>63</sup> ; LUBW <sup>64</sup> ; WB <sup>65</sup> ; LBAW <sup>66</sup> ; MKUEM <sup>67</sup> ; LUBN <sup>68</sup> ; BFG <sup>69</sup>
Denmark	DK	1,000	ODA <sup>70</sup>
Estonia	EE	67	GRDC <sup>16</sup>
Spain	ES	1,440	CEDEX <sup>71</sup>
Finland	FI	669	FEI <sup>72</sup>
France	FR	4,968	BanqueHydro <sup>73</sup>
Great Britain	GB	671	NRFA <sup>74</sup>
Greece	GR	31	GRDC <sup>16</sup> ; OHIN <sup>75</sup> ; HCRM <sup>76</sup>
Croatia	HR	317	DHZ <sup>77</sup>
Hungary	HU	98	GRDC <sup>16</sup> ; OVF <sup>78</sup>
Ireland	IE	464	EPA <sup>79</sup> ; OPW <sup>80</sup>
Iceland	IS	111	LamaH-Ice <sup>12</sup>
Italy	IT	767	GRDC <sup>16</sup> ; ISPRA <sup>81</sup> ; APC Abruzzo <sup>82</sup> ; CFRA Valle d'Aosta <sup>83</sup> ; ARPAE Emilia-Romagna <sup>84</sup> ; ARPA: Umbria <sup>85</sup> , Sardegna <sup>86</sup> , Lombardia <sup>87,88</sup> , Toscana <sup>89</sup> , Piemonte <sup>90</sup> ; ARPAL Liguria <sup>91</sup> ; ARPAV Veneto <sup>92</sup> ; SPRUD Trentino <sup>93</sup>
Lithuania	LT	76	GRDC <sup>16</sup>
Luxembourg	LU	19	NGGL <sup>94</sup>
Latvia	LV	61	GRDC <sup>16</sup>
Moldova	MD	2	GRDC <sup>16</sup>
Macedonia	MK	1	GRDC <sup>16</sup>
N. Ireland	NI	51	NRFI <sup>74</sup>
Netherlands	NL	17	RWS <sup>95</sup>
Norway	NO	189	NVE <sup>96</sup>
Poland	PL	1,287	IMGW-PIB <sup>97</sup>
Portugal	PT	280	SNIRH <sup>98</sup>
Romania	RO	18	GRDC <sup>16</sup>
Serbia	RS	18	GRDC <sup>16</sup>
Russia	RU	98	GRDC <sup>16</sup>
Sweden	SE	290	SMHI <sup>99</sup>
Slovenia	SI	117	ARSO <sup>100</sup>
Slovakia	SK	21	GRDC <sup>16</sup>
Turkey	TR	28	GRDC <sup>16</sup>
Ukraine	UA	21	GRDC <sup>16</sup>

820  
821

**Table 1.** Overview of streamflow time series data available per country/region, with information about number of stations and data providers.

Quality flag (gauge)	Criterion
A	More than 95% of the gauge records flags are “reliable”
B	More than 95% of the gauge records flags are “reliable” or “no-flag”
C	Less than 10% of the gauge records flags are “missing”
D	Less than 20% of the gauge records flags are “missing”
E	More than 20% of the gauge records flags are “missing”

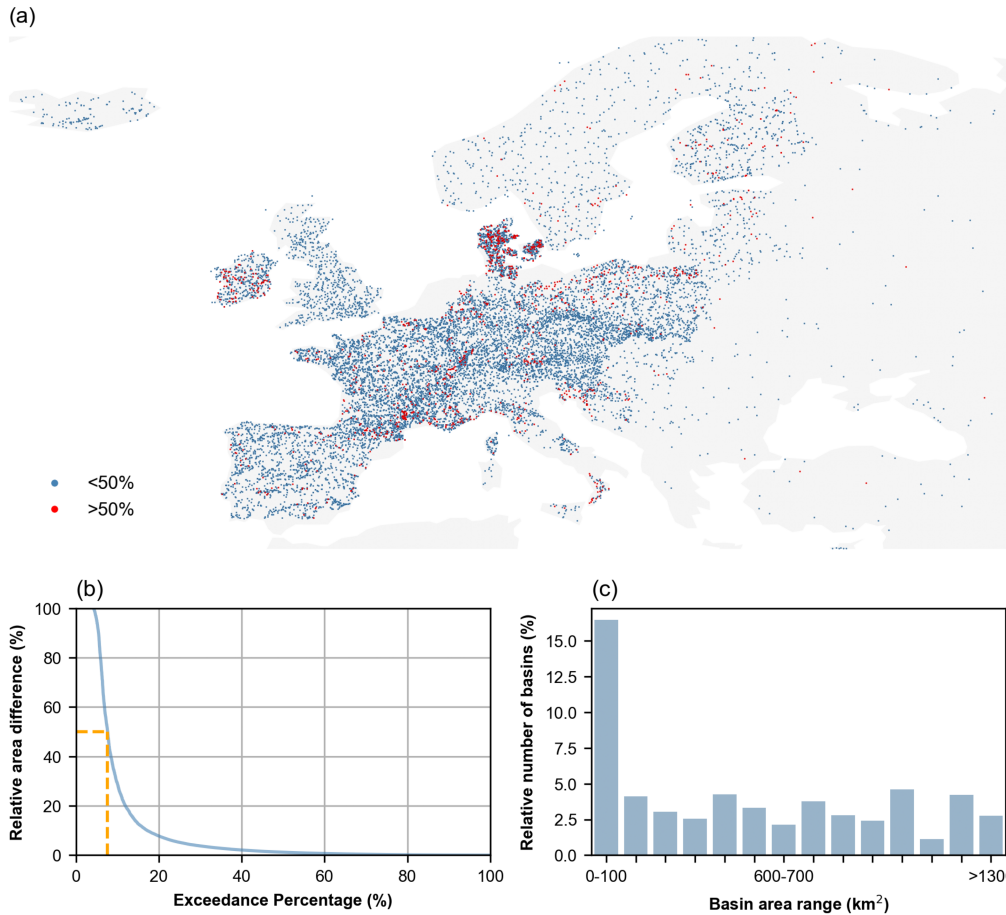
822 **Table 2.** Criteria used for the quality assessment of the streamflow gauges as in Chen, 2023<sup>100</sup>. When  
823 one station met multiple criteria simultaneously, the highest-level flag was applied.



824 **Figure 3.** (a) Histogram of the streamflow data points according to their four data quality flags and (b)  
825 Histogram of the number of gauges according to their integrated data quality flag.  
826

Basin area quality flag	Number of gauges	Description
0	12,801	$ A_{rel} $ below 10%.
1	164	$ A_{rel} $ below 10% after moving the gauge location.
2	1,037	$ A_{rel} $ above 10% or no reported area available, but delineation visually compared to other delineations from down and upstream gauges labelled “0”, Google Maps satellite imagery and to the EU-Copernicus River network.
3	369	$ A_{rel} $ above 10% or no reported area available, but delineation visually compared to Google Maps satellite imagery and to the EU-Copernicus River network.
4	343	$ A_{rel} $ above 30% or no reported area available, but delineation compared to EU-Copernicus River network.
5	68	$ A_{rel} $ above 10% or no reported area available, and delineation manually adjusted using EU-Copernicus in addition to MERIT-Hydro.
6	11	Similar to “5”, but still with $ A_{rel} $ above 30% or no reported area available.
888	64	$ A_{rel} $ above 10% or no reported area available, but location in areas under high human influence, such as canalization and water exports and in karstic regions.
999	2,273	$ A_{rel} $ above 10% or no reported area available, and delineation eventually not accepted after visual inspection.

827 **Table 3.** Description of the catchment area quality flags adopted for the current catchment delineations  
828 and overview of the number of catchments per group.



829  
830  
831  
832  
833  
834

**Figure 4.** (a) Relative absolute area difference  $|A_{rel}|$  above 50% (in red) and below 50% (in blue). (b) Exceedance percentage of the  $|A_{rel}|$ ; the orange line marks the exceedance percentage corresponding to a  $|A_{rel}|$  of 50%. (c) Bar plots showing the relative number of basins with areas above 50% for different basin area ranges (e.g., 0-100 km<sup>2</sup>, 100-200 km<sup>2</sup>, and >1,300 km<sup>2</sup>) relative to the total number of basins in each range. Basemap from GeoPandas<sup>50</sup>.

Variable	Description	Units	Resolution
mean	Mean daily streamflow.	mm day <sup>-1</sup>	W, M, S and Y
std	Standard deviation of the daily streamflow.	mm day <sup>-1</sup>	W, M, S and Y
cv	Coefficient of the variation of the daily streamflow.	-	W, M, S and Y
min	Minimum daily streamflow.	mm day <sup>-1</sup>	W, M, S and Y
max	Maximum daily streamflow.	mm day <sup>-1</sup>	W, M, S and Y
min7	Minimum 7-day streamflow.	mm day <sup>-1</sup>	M, S and Y
max7	Maximum 7-day streamflow.	mm day <sup>-1</sup>	M, S and Y
p_{10, 20, 30, 40, 50, 60, 70, 80, 90}	Percentile values of the daily streamflow.	mm day <sup>-1</sup>	S and Y
iqr	Interquartile range of the daily streamflow (P75 minus P25)	mm day <sup>-1</sup>	W, M, S and Y
ct	Centre timing, which corresponds to the day of the year (doy) at which 50 % of the annual flow is reached.	day	Y
doymax	The day of the year (doy) at which the minimum streamflow occurred.	day	Y
doymax	The day of the year (doy) at which the minimum streamflow occurred.	day	Y
doymax7	The day of the year (doy) at which the minimum 7-day streamflow occurred.	day	Y
doymax7	The day of the year (doy) at which the maximum 7-day streamflow occurred.	day	Y
gini	Gini coefficient	-	Y

835  
836

**Table 4.** Set of dynamic streamflow time series indices computed and made available at the present dataset.

Signature	Unit	Description
q_mean	mm day <sup>-1</sup>	Mean daily streamflow.
runoff_ratio	-	Ratio of mean daily streamflow to mean daily precipitation.
q_elas_Sankarasu bramanian	-	Streamflow precipitation elasticity. It represents the sensitivity of streamflow to changes in precipitation at the annual timescale computed using Eq. (7) in Sankarasubramanian, 2001 <sup>101</sup> , the last element being P/Q not Q/P
slope_sawicz	-	Slope of the flow duration curve computed using Eq. (3) in Sawicz, 2011 <sup>102</sup>
baseflow_index		Ratio of mean daily baseflow to mean daily streamflow, hydrograph separation performed using the Ladson, 2013 <sup>103</sup> digital filter.
hfd_mean	day of year	Mean half-flow date. It represents the date on which the cumulative streamflow reaches half of the annual discharge.
hfd_std	day of year	Standard deviation of the mean half-flow dates.
q_5	mm day <sup>-1</sup>	5 % flow quantile, which represents low flows.
q_95	mm day <sup>-1</sup>	95 % flow quantile, which represents high flows.
hq_freq	days yr <sup>-1</sup>	Frequency of Q > 9 times the median daily flow.
hq_dur	days	Average duration of flow events of consecutive days > 9 times the median daily flow.
lq_freq	days yr <sup>-1</sup>	Frequency of Q < 0.2 times the median daily flow.
lq_dur	days	Average duration of flow events of consecutive days < 0.2 times the median daily flow.
zero_q_freq	-	Frequency of days with Q = 0
p_mean	mm day <sup>-1</sup>	Mean daily precipitation.
pet_mean	mm day <sup>-1</sup>	Mean daily potential evapotranspiration (PET).
aridity	-	Ratio between PET and precipitation.
p_seasonality	-	Seasonality and timing of precipitation, which was estimated using the precipitation and temperature time series.
frac_snow	-	Fraction of precipitation falling as on days colder than 0 °C.
hp_freq	days yr <sup>-1</sup>	Frequency of P > 5 times the median daily precipitation (high precipitation).
hp_dur	days	Average duration of periods with consecutive high precipitation events.
hp_time	season	Season during most high precipitation events occur (e.g., Fall, Winter, Summer or Spring).
lp_freq	days yr <sup>-1</sup>	Frequency of P events < 1 mm day <sup>-1</sup> (dry days).
lp_dur	days	Average duration of periods with consecutive dry days.
lp_time	season	Season during most dry days occur (e.g., Fall, Winter, Summer or Spring).
num_years_{hydr o, climatic}	-	Number of years with hydrological or meteorological observations used for the signatures' computation.
start_date_{hydro , climatic }	date	First date with with hydrological or meteorological observations used for the signatures' computation.
end_date_{hydro, climatic }	date	Last date with hydrological or meteorological used for the signatures' computation.

837  
838  
839  
840

**Table 5.** Set of static hydro-climatic signatures. The hydrological year considered in this study starts at 1st of October and goes until the 30th of September. Unlike streamflow indices, these signatures are static, each represented by a single value calculated for the available data for the period from 1950 to 2022.

Group	Attribute	Description	Unit	Source
Meteorology	p_mean	Total mean daily precipitation measured as the height of the equivalent liquid water in a square meter.	mm day <sup>-1</sup>	E-OBS <sup>19</sup>

Group	Attribute	Description	Unit	Source
	t_{mean, min, max}	Daily mean, minimum and maximum air temperature measured near the surface.	°C	
	sp_mean	Mean air pressure at sea level.	hPa	
	rh_mean	Daily mean relative humidity measured near the surface.	%	
	ws_mean	Daily mean wind speed at 10-meter height.	ms <sup>-1</sup>	
	swr_mean	The flux of shortwave radiation (also known as solar radiation) measured at the Earth's surface.	Wm <sup>-2</sup>	
	pet_mean	Potential evapotranspiration was estimated using the Hargreaves equation <sup>44</sup> .	mm day <sup>-1</sup>	derived
	stations_num_{p_mean, t_mean, t_min, t_max, sp_mean, rh_mean, ws_mean, swr_mean}	Number of weather stations measuring the given variable within the catchment boundary assuming a 10 km buffer.	-	E-OBS <sup>19</sup>
stations_dens_{p_mean, t_mean, t_min, t_max, sp_mean, rh_mean, ws_mean, swr_mean}	Weather stations density for the given variable within the catchment boundary.	Stations km <sup>-2</sup>		

841  
842  
843

**Table 6.** Meteorological catchment attributes at daily resolution from 1950 to 2022. These attributes are aggregated over individual catchment boundaries. The table details both the time series variables and the information regarding the number of stations and their density.

Group	Attribute	Description	Unit	Source
Topography	ele_mt_{max, mean, min }	Mean, minimum and maximum elevation.	m	MERIT-Hydro <sup>22,25</sup>
	slp_dg_mean	Mean terrain slope.	°	
	flat_area_fra	Percentage of area with slope <3°.	%	
	steep_area_fra	Percentage of area with slope >15°.	%	
	elon_ratio	Derived elongation ratio <sup>104</sup>	-	
	strm_dens	Stream density, ratio of lengths of streams and the catchment area.	1000 Km km <sup>-2</sup>	
Soils*	root_dep	Depth available for roots.	cm	European Soil Database Derived data (ESDD) <sup>29-31</sup>
	soil_tawc	Total available water content.	mm	
	soil_fra_{sand, silt, clay, grav}	Sand, silt, clay and gravel fraction of soil material.	%	
	soil_bd	Bulk density.	g cm <sup>-3</sup>	
	oc_fra	Fraction of organic material.	%	
Geology	lit_fra_{class}	Percentage of each lithological class aggregated over the catchment.	%	Global Lithological Map Database (GLiM) <sup>20</sup>
	lit_dom	Lithological dominant class.	Classes (n=16)	
	tot_area	Percentage of the catchment area covered by GLiM.	%	
	bedrk_dep	Depth to bedrock.	m	Pelletier, 2016 <sup>21</sup>
Hydrology	dam_num	Number of dams upstream.	-	Georeferenced global Dams and Reservoirs <sup>23</sup>
	res_num	Number of reservoirs upstream.		
	dam_yr{first, last}	First and last years of dam's construction.	-	
	res_tot_sto	Total upstream storage volume.	10 <sup>6</sup> m <sup>3</sup>	
	lakes_num	Number of lakes upstream.	-	HydroLakes <sup>46</sup>

Group	Attribute	Description	Unit	Source
	lakes_tot_area	Total area covered by lakes upstream.	Km <sup>2</sup>	
	lakes_tot_vol	Total upstream volume.	10 <sup>6</sup> m <sup>3</sup>	
Vegetation	ndvi_{month, mean}**	Mean NDVI over the catchment area.	-	MODIS <sup>32</sup>
	lai_{month, mean}**	Mean LAI over the catchment area.	-	MODIS <sup>33</sup>
Landcover	sno_cov_{month, mean}**	Mean snow cover percentage over the catchment area.	%	MODIS <sup>28</sup>

844  
845  
846  
847  
848  
849

**Table 7.** Set of static catchment attributes included in the present dataset.

\* All soil attributes were aggregated by mean, max, min, P05, P25, med, P75 and P90, which sums to a total of 64 variables.

\*\* NDVI, LAI and snow cover attributes were aggregated considering the total mean and the month of the year (January = 01 to December = 12) mean from the period between 01.01.2001 to 31.12.2022, which means that each attribute has 13 variables here referred as static since not shown in a time series format.

Group	Attribute	Description	Unit	Source
Vegetation	ndvi_mean	Monthly and yearly NDVI.	-	MODIS <sup>32</sup>
	lai_mean	Monthly and yearly LAI.	-	MODIS <sup>33</sup>
Landcover	sno_cov_mean	Monthly and yearly snow cover percentage time series.	%	MODIS <sup>28</sup>
	irrig_area_{yr}	10/5-year resolution total area equipped for irrigation.	km <sup>2</sup>	AEI_EARTHSTAT_IR product from HID <sup>27</sup>
	tot_area_{year}	Fraction of the catchment area covered by the Corine product.	-	CORINE <sup>26</sup>
	lulc_dom_{year}	Land cover majority class for 1990, 2000, 2006, 2012 and 2018.	Classes (n=44)	
	lulc_{year}_{class}	Fraction of each landcover class aggregated over the catchment for 1990, 2000, 2006, 2012 and 2018.	-	

850  
851  
852

**Table 8.** Set of the temporal catchment landscape attributes. Vegetation and snow cover attributes have a monthly and yearly resolution from 2001-2022. The irrigation has a variable window resolution of 10-5-years from 1900-2005.

Attribute name	Description
provider_id	Unique code used to refer the <i>basin_id</i> to their respective data provider
code_basins	Code shown in the first two-four digits of the <i>basin_id</i> of their respective catchments
provider_country	Country name of the data provided.
country_code	Country code of the data provided (e.g., PT for Portugal or AT for Austria).
provider_name	Name of the data provider.
license_redistribution	Type of redistribution license.
platform	Platform where the dataset is available. Either a website, or via contact request.
num_stations	Total number of streamflow stations available on the platform as of the date the catalogue data was derived.
start_date	Date of the first available streamflow measurement at the date of request/download.
end_date	Date of the last available streamflow measurement at the date of request/download.
website	Link to the official website of the data provider.
source_license	Link where the users can get further information regarding license and terms of use (when available).
source_streamflow	Link to the streamflow data provider website.
source_gauges_infos	Link to the official source where the gauges information is available (location, river and name).
references	Formal reference for citing the streamflow data.
observations	Extra information when needed to provide further guidance to the users.

download_method	Method of download available at the moment of publication. This specifies if users should download the data manually and individually, or if there is an official API, a provided code, or if a contact form is necessary to request the records.
-----------------	---

853

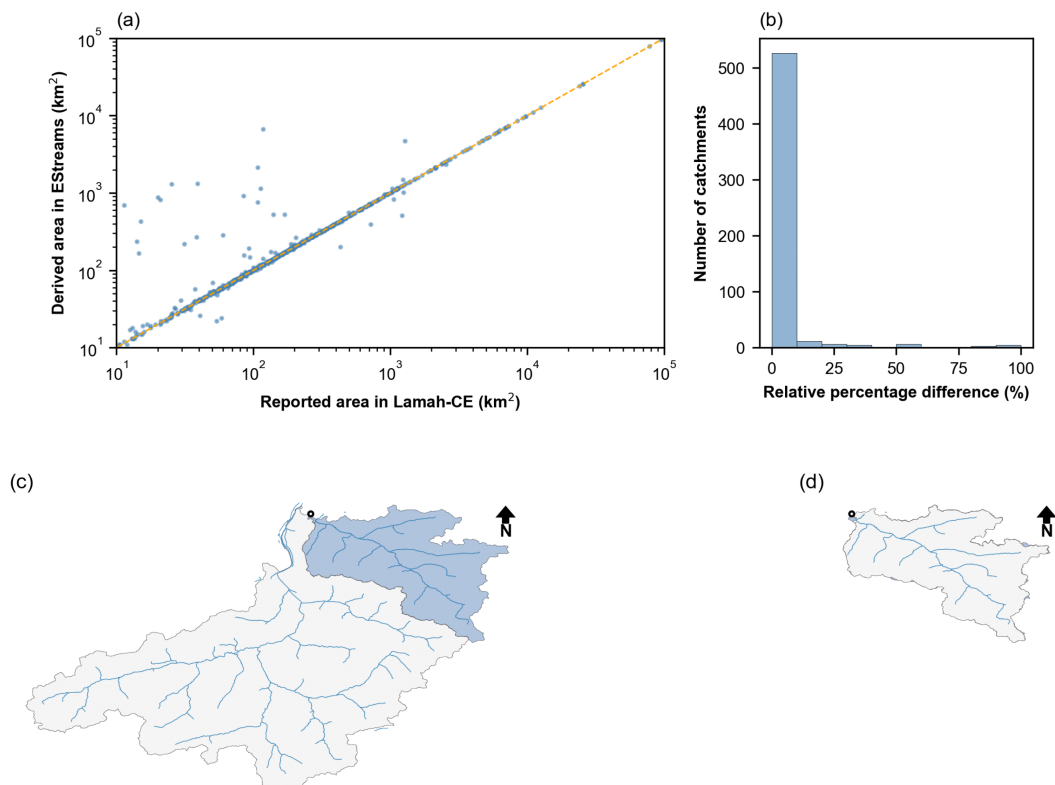
**Table 9.** Attribute fields included in the European Streamflow Catalogue provided.

Attribute name	Description
basin_id	An 8-digit code defined by this work.
gauge_id	The official code available by the data source, which can be used to retrieve records directly from the data providers.
gauge_name	The official name of the station provided by the data source*.
gauge_country	Country code where the gauge is located.
gauge_provider	Data source code aligned with the catalogue.
river	The name of the river provided by the data source*.
lon_snap	Longitude of the gauge in WGS84 original or moved.
lat_snap	Latitude of the gauge in WGS84 original or moved.
lon	Longitude of the gauge in WGS84 provided by the data source.
lat	Latitude of the gauge in WGS84 provided by the data source.
elevation	The official gauge elevation reported by the data provider*.
area_official	The official area reported by the data provider ( $A_{\text{official}}$ )*.
area_estreams	The area (in km <sup>2</sup> ) derived from the current delineation methodology ( $A_{\text{Estreams}}$ ).
area_flag	A quality flag for the current area computation as reported in <b>Table 3</b> .
area_rel	The percentual (%) relative difference between the derived and the reported area, relative to the reported area, as defined by <b>Eq. (1)</b> .
start_date	First date with valid observations as of the date the data was accessed.
end_date	Last date with valid observations as of the date the data was accessed.
num_years	Number of years with valid data.
num_months	Number of months with valid data.
num_days	Number of days with valid data.
num_continuous_days	Maximum number of days between the <i>start_date</i> and <i>end_date</i> with no gaps.
num_days_gaps	Number of days with gaps between the <i>start_date</i> and <i>end_date</i> .
num_days_reliable	Number of days with data classified as “reliable” from the respective provider.
num_days_noflag	Number of days with data without a quality flag provided by the respective provider.
num_days_suspect	Number of days with data classified as “suspect” from the respective provider.
gauge_flag	Quality flag of the respective streamflow gauge as reported in <b>Table 2</b> .
duplicated_suspect	If it is the case, <i>basin_id</i> of the gauge suspect of being a duplicate with this gauge.
watershed_group	A number assigning to which main watershed is the gauge belongs to, e.g., all gauges within the Rhine watershed are assigned the number 1.
gauges_upstream	The number of unique gauging stations upstream of the given gauge. This count includes the basin itself but excludes any duplicate stations. This means that if one gauge has a duplicate, the count considers only one gauge.
nested_catchments	A list of all nested catchments within the given basin. This list includes the basin itself and may differ from the total number in <i>gauges_upstream</i> because it includes all gauges, retaining any duplicates within the same list.

854

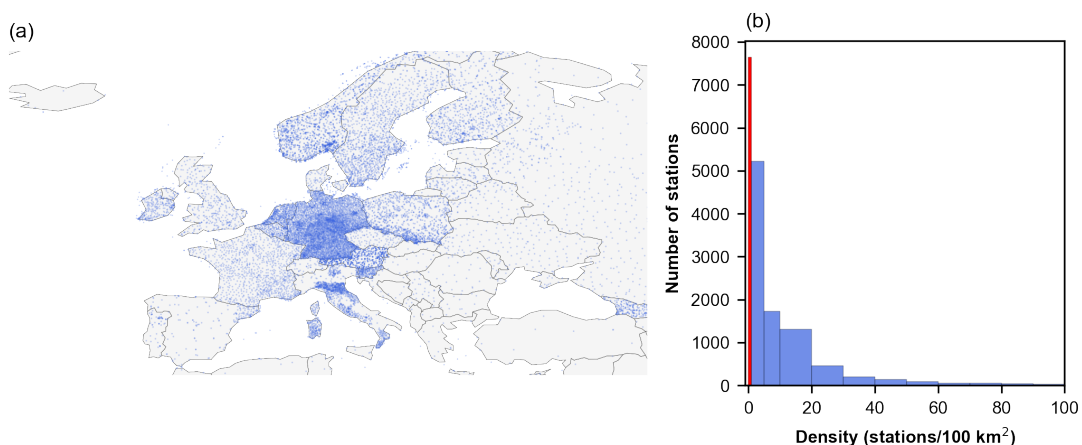
**Table 10.** Description of the attributes of the streamflow gauges' layer.

855 \*These are information seldom not available from official sources.

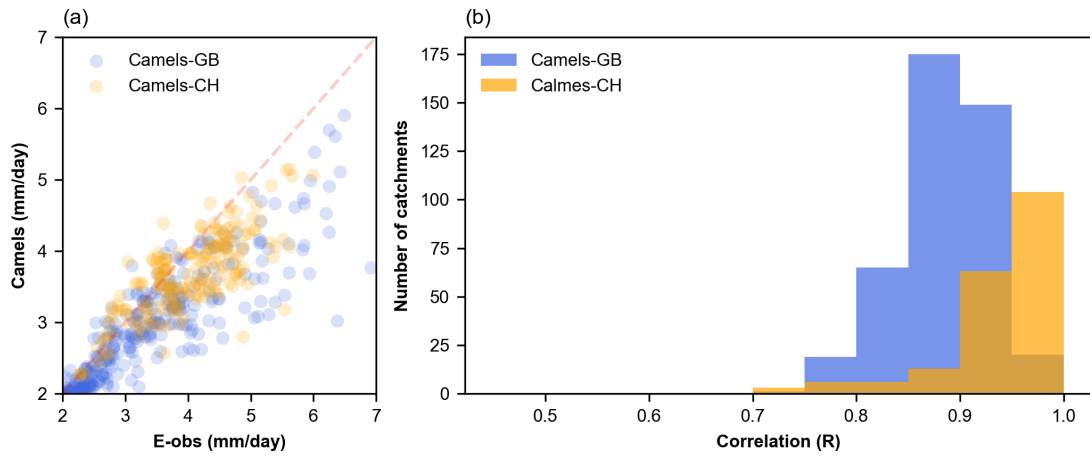


856

857 **Figure 5.** (a) Comparison of catchment boundary areas reported LamaH-CE<sup>8</sup> against those delineated in  
 858 this study. Both axes are presented in logarithmic scale to enhance visualization. (b) Histogram  
 859 illustrating the  $|A_{rel}|$  between the two sources of data. Most catchments exhibit  $|A_{rel}|$  below 10%.  
 860 Catchment AT00009 (EStreams) delineations are displayed (c) prior to manual adjustment of the outlet  
 861 location and (d) following manual adjustment.



862 **Figure 6.** (a) Overview of the spatial distribution of the stations used to derive the precipitation time series  
 863 grided data available at E-OBS<sup>19</sup>. (b) Histogram of the stations per catchment. Due to the high  
 864 distribution of densities the bins are not evenly spaced, and the first bin (in red) corresponds to the  
 865 threshold of one station per 100 km<sup>2</sup>. Basemap from GeoPandas<sup>50</sup>.  
 866



867  
 868  
 869  
 870  
 871

**Figure 7.** (a) Scatter plot of the long-term mean daily precipitation (1950-2022) considering the precipitation forcing time series derived from E-OBS<sup>19</sup> and the provided in CAMELS-CH<sup>7</sup> and CAMELS-GB<sup>6</sup> and (b) Histogram of the correlation coefficient between the two data sources. The plots only show catchments with areas above 100 km<sup>2</sup>.